F1000Research

Check for updates

RESEARCH ARTICLE

REVISED TOP2DFVT: An Efficient Matlab Implementation for Topology Optimization based on the Finite-Volume Theory [version 2; peer review: 3 approved]

Marcelo Araujo, Arnaldo Santos Júnior, Romildo Escarpini Filho, Eduardo Lages (iD), Marcio Cavalcante (iD)

Universidade Federal de Alagoas, Maceió, State of Alagoas, Brazil

Abstract

The finite-volume theory has shown to be numerically efficient and stable for topology optimization of continuum elastic structures. The significant features of this numerical technique are the local satisfaction of equilibrium equations and the employment of compatibility conditions along edges in a surface-averaged sense. These are essential properties to adequately mitigate some numerical instabilities in the gradient version of topology optimization algorithms, such as checkerboard, mesh dependence, and local minima issues. Several computational tools have been proposed for topology optimization employing analysis domains discretized with essential features for finite-element approaches. However, this is the first contribution to offer a platform to generate optimized topologies by employing a Matlab code based on the finite-volume theory for compliance minimization problems. The Top2DFVT provides a platform to perform 2D topology optimization of structures in Matlab, from domain initialization for structured meshes to data post-processing. This contribution represents a significant advancement over earlier publications on topology optimization based on the finite-volume theory, which needed more efficient computational tools. Moreover, the Top2DFVT algorithm incorporates SIMP and RAMP material interpolation schemes alongside sensitivity and density filtering techniques, culminating in a notably enhanced optimization tool. The application of this algorithm to various illustrative cases confirms its efficacy and underscores its potential for advancing the field of structural optimization.

Open Peer Review

Approval Status ✓ ✓ ✓

	1	2	3
version 2 (revision) 22 Oct 2024	✓ view	✓ view	✓ view
version 1 16 Jul 2024	? view	? view	? view

1. **Yingjun Wang** (iD), South China University of Technology, Guangzhou, China

2. **Minh Ngoc Nguyen** (iD), Duy Tan University, Ho Chi Minh city, Vietnam

3. **Volnei Tita** (iD), University of Sao Paulo, Sao Paulo, Brazil

Any reports and responses or comments on the article can be found at the end of the article.

Keywords

topology optimization, compliance minimization problem, finite-
volume theory, Matlab.

Corresponding author: Marcio Cavalcante (marcio.cavalcante@ceca.ufal.br)

Author roles: Araujo M: Conceptualization, Data Curation, Investigation, Methodology, Software, Validation, Visualization, Writing –
Original Draft Preparation; **Santos Júnior A**: Data Curation, Investigation, Methodology, Software, Supervision, Validation, Writing –
Review & Editing; **Escarpini Filho R**: Formal Analysis, Investigation, Software, Supervision, Writing – Review & Editing; **Lages E**: Data
Curation, Funding Acquisition, Investigation, Methodology, Software, Supervision, Writing – Review & Editing; **Cavalcante M**:
Conceptualization, Formal Analysis, Funding Acquisition, Investigation, Methodology, Project Administration, Resources, Supervision,
Writing – Review & Editing

How to cite this article: Araujo M, Santos Júnior A, Escarpini Filho R *et al.* **TOP2DFVT: An Efficient Matlab Implementation for
Topology Optimization based on the Finite-Volume Theory [version 2; peer review: 3 approved]** F1000Research 2024, **13**:805
https://doi.org/10.12688/f1000research.150945.2

First published: 16 Jul 2024, **13**:805 https://doi.org/10.12688/f1000research.150945.1

> **REVISED** **Amendments from Version 1**
>
> Significant updates were made to enhance clarity and address the reviewers' comments. Although no changes were made to the abstract, fourteen textual modifications were introduced in the main body of the manuscript, including clarifications regarding the local stiffness matrix and a discussion on the impact of memory preallocation, outlining the trade-offs between computational speed and memory usage.
>
> Five new figures were incorporated into the manuscript. One figure presents a flowchart detailing the algorithm's workflow, providing a clearer understanding of the methodology. A second figure was added to present the convergence analysis of the SIMP and RAMP methods with and without filtering. The sensitivity filter accelerates convergence by smoothing the local response, while the density filter reduces thin bars but requires more iterations and higher computational costs. The RAMP method provides gradual convergence and smaller discontinuities in the continued penalization scheme, in contrast with the SIMP method, which is also more sensitive to mesh refinement.
>
> Three added figures show optimized topologies obtained using the top99neo algorithm for comparison with those previously generated using the Top2DFVT code, illustrating the differences in mesh dependency between the methods, with the Top2DFVT demonstrating a lower sensitivity to mesh refinement. A comparison of computational efficiency between the Top2DFVT and top99neo algorithms was introduced in the text, with the Top2DFVT exhibiting a higher computational cost in some scenarios due to the larger number of degrees of freedom and offering advantages in terms of numerical stability.
>
> The data in the tables were not changed, and a reference suggested by one of the reviewers was included in the introduction to contextualize previous work on topology optimization of anisotropic composites.
>
> These revisions ensure that the manuscript comprehensively addresses the reviewers' concerns, enhancing the technical depth and clarity while maintaining the integrity of the original data and abstract.
>
> **Any further responses from the reviewers can be found at the end of the article**

1. Introduction

In structural engineering, topology optimization is a technique that searches for the best material distribution inside an analysis domain based on an objective function and one or more constraints (Bendsøe and Sigmund, 2003). Therefore, topology optimization allows for the discovery of innovative and high-performance structural designs, which attracted the interest of mathematicians and engineers (Liu and Tovar, 2014). With the progressive development of computer technology and computational mechanics over the last decades, the structural topology optimization tools have gradually experienced improvements that allow the solution of medium and large-scale problems. In addition, topology optimization has become an effective strategy for generating innovative forms for additive manufacturing, architectural design, and engineering (Zhuang et al., 2023). In general, compliance evaluation has played an important role in topology optimization algorithms. Since the pioneer work of Michell (1904), who derived the optimality criteria (OC) method, and the reconstruction proposed by Bendsøe and Kikuchi (1988), a great part of the advances in topology optimization has been achieved by employing methodologies based on structural compliance minimization problems. Some studies on this field can still be found in Liu et al. (2023), Yi et al. (2023), Lee et al. (2023), Arruda et al. (2022), Bouajila et al. (2021), and Ferrari and Sigmund (2020). Recent advances in topology optimization have expanded to include anisotropic composites, optimizing both material distribution and fibre orientation. Almeida et al. (2023) introduced a framework for concurrent optimization of topology and fibre orientation in 3D-printed fibre-reinforced composites, effectively minimizing compliance. This approach, particularly for materials like onyx, enhances stiffness and strength, offering significant benefits for additive manufacturing of high-performance and lightweight structures.

In topology optimization algorithms, the interest is in determining whether we should put material or not, which generates a "black and white" design. Therefore, the structural material distribution is obtained by a binary "0-1", where 0 indicates void and 1 indicates the presence of material. However, this kind of topology optimization algorithms lead to an integer programming problem, which has revealed to be an unfeasible approach for large scale topology optimization problems. An alternative approach is the SIMP (*Solid Isotropic Material with Penalization*) method, which has been extensively used due to its versatility, convergence, and ease implementation (Rozvany, 2009). In this approach, the material properties can be evaluated inside each element of the discretized domain, and the design variables are the elements' relative densities. Therefore, the mechanical properties are modeled by the material relative density raised to a penalty factor that penalizes their intermediate values. Another interpolation scheme to penalize intermediate values of relative density is the RAMP (*Rotational Approximation of Material Properties*) method proposed by Stolpe and Svanberg (2001), which employs a concave penalty function to suppress these intermediate values in the objective function. Unlike the SIMP method, the RAMP model presents non-zero sensitivity at zero density, so this model is especially efficient to remedy some numerical difficulties presented in problems with very low densities (Deaton and Grandhi, 2014).

Different authors have developed educational algorithms to design optimized topologies in the last two decades. The trailblazer top99 educational code written in Matlab proposed by Sigmund (2001) had promoted important impacts in the topology optimization field, such as teaching of topology optimization tools in undergraduate courses, building simple code for new researchers, and pioneering a new popular category of publications in the structural optimization field: educational articles self-containing compact codes for teaching and research (Zhou and Sigmund, 2021). Beyond the well-known top99 Matlab code, several computer tools for Matlab and other platforms are available, such as PETSc by Smit et al. (2021) and Aage et al. (2015) for Python; TopOpt app by Aage et al. (2013) for language C; Stutz et al. (2022), Aage and Lazarov (2013), and Borrvall and Petersson (2001) for C++ language; Liu et al. (2005) for Femlab; and Sokół (2011) for Mathematica. However, a significant part of the proposed educational algorithms for topology optimization is written in Matlab language, as top99neo by Ferrari and Sigmund (2020), an 88-line code for parametrized level-set method by Wei et al. (2018), top88 by Andreassen et al. (2011), top3d by Liu and Tovar (2014), PolyTop by Talischi et al. (2012), HoneyTop90 by Kumar (2023), a 115-line code for multi-material topology optimization by Tavakoli and Mohseni (2014), and GRAND by Zegard and Paulino (2014).

In the top99 topology optimization code, the performance of several operations can be increased by exploiting the strengths of Matlab, such as loop vectorization and memory preallocation, and by restructuring the program, as moving portions of code out of the optimization loop so they would be executed once (Andreassen et al., 2011). Therefore, Andreassen et al. (2011) have proposed an 88-line code in Matlab for compliance minimization by allocating these computational features (top88), which has substantially improved the computational performance of the optimization algorithm. Later, Liu and Tovar (2014) have extended this algorithm to three-dimensional problems by also placing other strategies for topology optimization of compliant mechanisms and heat conduction problems. With the evolution of topology optimization research field and Matlab, the top88 code has become outdated, which has motivated the publication of the new generation of the top99 code (top99neo) by Ferrari and Sigmund (2020), making some improvements inmet the assembly operations, accelerating the Optimality Criteria (OC) method, filters implementation, and extending to three-dimensional structures.

Araujo et al. (2020a,b) propose applying the finite-volume theory for topology optimization considering compliance minimization. This theory has been shown to be numerically stable for optimization problems, especially its checkerboard-free property, even when a non-filtering technique is employed. Numerical stability is an essential feature of the finite-volume theory applied in topology optimization tools to obtain more reliable optimized topologies. Also, this technique has shown to be well suitable method for elastic stress analysis in solid mechanics, investigations of its numerical efficiency can be found in Araujo et al. (2021), Cavalcante et al. (2007a,b, 2008) and Cavalcante and Pindera (2012a,b). The satisfaction of equilibrium equations at the subvolume level, concomitant to kinematic and static continuities established in a surface-averaged sense between common faces of adjacent subvolumes, are features that distinguish the finite-volume theory from the finite-element method. Thus, in the finite-volume theory, the connections between adjacent subvolumes occur through subvolumes' faces, which is more likely from the continuum mechanics point of view.

This contribution provides a new topology optimization tool for the analysis of 2D structures using the Matlab language, which starts from domain discretization and continues until data is post-processed. In addition, based on the authors' knowledge, this is the first time a platform for optimizing structures using the finite-volume theory can be applied to medium and large-scale problems, besides obtaining checkerboard-free and mesh-independent designs. The topology optimization tool also incorporates the SIMP and RAMP methods and the sensitivity and density filters. Employing a symmetric modified stiffness matrix also represents an advance since it accelerates the algorithm and establishes a relation between resultant forces and displacements instead of tractions and displacements, which are energetically conjugated static and kinematic quantities. These improvements have dramatically reduced the computational cost and solved the oscillatory phenomenon issue through the RAMP approaches, especially compared with the results in Araujo et al. (2020a). More details about the implementation can be found in the GitHub link (https://github.com/fvt7782/Top2DFVT).

2. Finite-volume theory

In general, the finite-volume theory employs the stress and displacement fields and imposes boundary and continuity conditions between adjacent subvolumes in an average-sense, which has guaranteed the checkerboard-free property discussed in Araujo et al. (2020a). Additionally, the differential equilibrium equations are locally satisfied in an average-sense (Araujo et al., 2021), and the displacement field in the subvolume is modeled by second-order polynomials defined in local coordinates (Cavalcante et al., 2007a). The presented formulation has its roots in the standard version of the finite-volume theory presented in Cavalcante and Pindera (2012a) for structured meshes formed by rectangular subvolumes. Fundamentally, the structural analysis problem involves mechanical quantities evaluation, as applied loads, internal
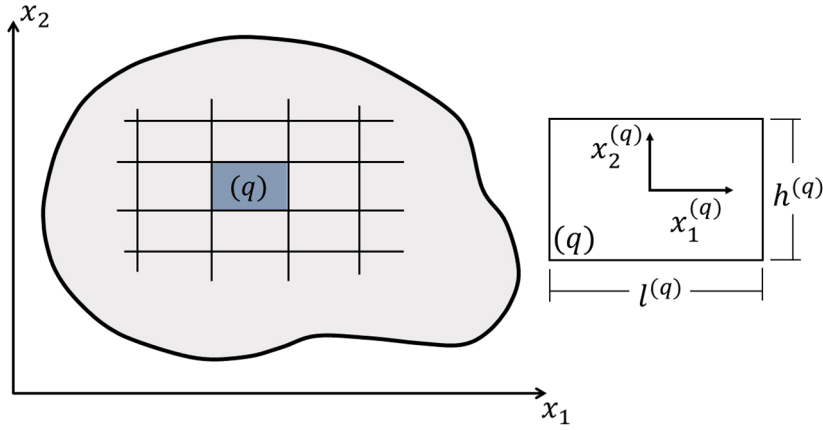
Figure 1. Discretized reference domain and global coordinate system (left) and subvolume and local coordinate system (right).

forces, displacements, and strains. The main objective is determining the stress and displacements when structural discretized domains are employed, where stress-strain relation can be easily expressed.

Figure 1 presents the analysis domain in $x_1 - x_2$ plane, which is discretized in N_q subvolumes. The subvolume dimensions are $l^{(q)}$ and $h^{(q)}$ for $q = 1, \ldots, N_q$, where $x_1^{(q)}$ and $x_2^{(q)}$ represent the local coordinate system. Following Cavalcante and Pindera (2012a), the displacement of a subvolume q can be approximated by an incomplete quadratic version of Legendre polynomial expansion in the local coordinate system as follows:

$$u_i^{(q)} = W_{i(00)}^{(q)} + x_1^{(q)} W_{i(10)}^{(q)} + x_2^{(q)} W_{i(01)}^{(q)} + \frac{1}{2}\left(3x_1^{(q)^2} - \frac{l^{(q)^2}}{4}\right)W_{i(20)}^{(q)} + \frac{1}{2}\left(3x_2^{(q)^2} - \frac{h^{(q)^2}}{4}\right)W_{i(02)}^{(q)}, \tag{1}$$

where $i = 1, 2$ and $W_{i(mn)}^{(q)}$ are unknown coefficients of the displacement field. Therefore, the surface-averaged displacement components of a generic subvolume are represented in Figure 2(a) and can be defined as

$$\begin{aligned}
\overline{u}_i^{(q,p)} &= \frac{1}{l^{(q)}} \int_{-\frac{l^{(q)}}{2}}^{\frac{l^{(q)}}{2}} u_i\left(x_1^{(q)}, \mp\frac{h^{(q)}}{2}\right) dx_1^{(q)}, \text{for } p = 1,3 \\
\overline{u}_i^{(q,p)} &= \frac{1}{h^{(q)}} \int_{-\frac{h^{(q)}}{2}}^{\frac{h^{(q)}}{2}} u_i\left(\pm\frac{l^{(q)}}{2}, x_2^{(q)}\right) dx_2^{(q)}, \text{for } p = 2,4
\end{aligned}. \tag{2}$$

Similarly, considering the application of Cauchy's law and the plane stress state, the surface-averaged traction components at the subvolume faces can be evaluated as

$$\begin{aligned}
\overline{t}_i^{(q,p)} &= \mp\frac{1}{l^{(q)}} \int_{-\frac{l^{(q)}}{2}}^{\frac{l^{(q)}}{2}} \sigma_{2i}\left(x_1^{(q)}, \mp\frac{h^{(q)}}{2}\right) dx_1^{(q)}, \text{for } p = 1,3 \\
\overline{t}_i^{(q,p)} &= \pm\frac{1}{h^{(q)}} \int_{-\frac{h^{(q)}}{2}}^{\frac{h^{(q)}}{2}} \sigma_{1i}\left(\pm\frac{l^{(q)}}{2}, x_2^{(q)}\right) dx_2^{(q)}, \text{for } p = 2,4
\end{aligned}, \tag{3}$$

where $\overline{t}_i^{(q,p)}$ are adequately represented in Figure 2(b).

Following Araujo et al. (2020a), the local system of equations for a generic subvolume can be established as

$$\overline{t}^{(q)} = K^{(q)}\overline{u}^{(q)}, \tag{4}$$

where $\overline{u}^{(q)} = \left[\overline{u}_1^{(q,1)}, \overline{u}_2^{(q,1)}, \overline{u}_1^{(q,2)}, \overline{u}_2^{(q,2)}, \overline{u}_1^{(q,3)}, \overline{u}_2^{(q,3)}, \overline{u}_1^{(q,4)}, \overline{u}_2^{(q,4)}\right]^T$ is the local surface-averaged displacement vector, $\overline{t}^{(q)} = \left[\overline{t}_1^{(q,1)}, \overline{t}_2^{(q,1)}, \overline{t}_1^{(q,2)}, \overline{t}_2^{(q,2)}, \overline{t}_1^{(q,3)}, \overline{t}_2^{(q,3)}, \overline{t}_1^{(q,4)}, \overline{t}_2^{(q,4)}\right]^T$ is the local surface-averaged traction vector, and $K^{(q)}$ is the local stiffness
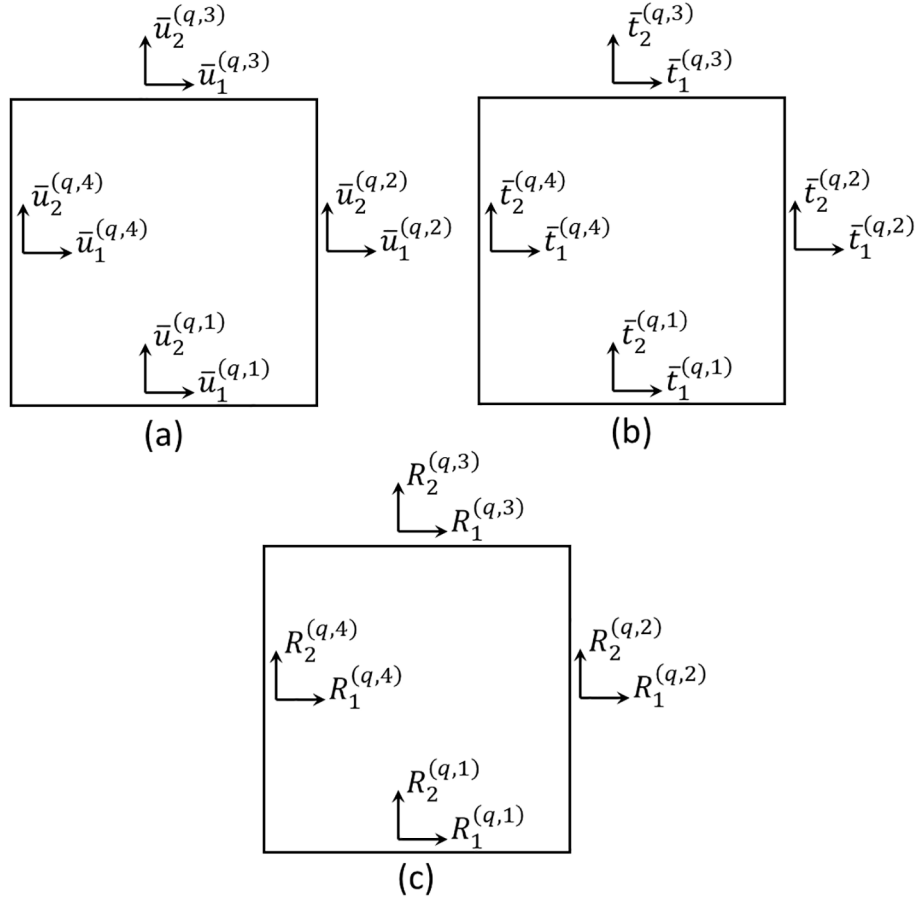
Figure 2. Degrees of freedom in a generic subvolume: (a) surface-averaged displacements, (b) surface-averaged tractions, and (c) resultant forces along edges.

matrix for a generic subvolume q. However, $K^{(q)}$ is a non-symmetric matrix, which increases the computational cost of topology optimization problems based on the finite-volume theory when compared to the same approaches based on the finite-element method. Additionally, the surface-averaged tractions are not energetically conjugated with the surface-averaged displacements along the subvolume faces, which leads the $K^{(q)}$ matrix to be more a pseudo stiffness matrix. Following Araujo et al. (2021), it can be defined a modified local system of equations in terms of resultant forces acting in the edges of a subvolume q, which are energetically conjugated with the surface-averaged displacements, as follows

$$\boldsymbol{R}^{(q)} = \overline{\boldsymbol{L}}^{(q)} \overline{\boldsymbol{t}}^{(q)} = \overline{\boldsymbol{L}}^{(q)} \boldsymbol{K}^{(q)} \overline{\boldsymbol{u}}^{(q)} = \overline{\boldsymbol{K}}^{(q)} \overline{\boldsymbol{u}}^{(q)}, \tag{5}$$

where $\overline{\boldsymbol{K}}^{(q)} = \overline{\boldsymbol{L}}^{(q)} \boldsymbol{K}^{(q)}$ is the modified local stiffness matrix, which is found to be a symmetric 8 by 8 matrix, $\boldsymbol{R}^{(q)} = \left[R_1^{(q,1)}, R_2^{(q,1)}, R_1^{(q,2)}, R_2^{(q,2)}, R_1^{(q,3)}, R_2^{(q,3)}, R_1^{(q,4)}, R_2^{(q,4)} \right]^T$ is the local resultant force vector, whose components are illustrated in Figure 2(c), and $\overline{\boldsymbol{L}}^{(q)}$ can be defined as

$$\overline{\boldsymbol{L}}^{(q)} = \begin{bmatrix} \boldsymbol{L}^{(q,1)} & \boldsymbol{0} & \boldsymbol{0} & \boldsymbol{0} \\ \boldsymbol{0} & \boldsymbol{L}^{(q,2)} & \boldsymbol{0} & \boldsymbol{0} \\ \boldsymbol{0} & \boldsymbol{0} & \boldsymbol{L}^{(q,3)} & \boldsymbol{0} \\ \boldsymbol{0} & \boldsymbol{0} & \boldsymbol{0} & \boldsymbol{L}^{(q,4)} \end{bmatrix} \quad \text{for} \quad \boldsymbol{L}^{(q,p)} = \begin{bmatrix} L_p^{(q)} & 0 \\ 0 & L_p^{(q)} \end{bmatrix}, \tag{6}$$

where $L_1^{(q)} = l^{(q)}$, $L_2^{(q)} = h^{(q)}$, $L_3^{(q)} = l^{(q)}$ and $L_4^{(q)} = h^{(q)}$ as illustrated in Figure 1.

Therefore, the modified global system of equations can be written as

$$\boldsymbol{R} = \overline{\boldsymbol{K}}\overline{\boldsymbol{u}}, \tag{7}$$

where $\overline{\boldsymbol{K}} = \sum_{q=1}^{N_q} \boldsymbol{Q}^{(q)^T} \overline{\boldsymbol{K}}^{(q)} \boldsymbol{Q}^{(q)}$ is the modified global stiffness matrix, obtained by summing the individual contribution of each subvolume of the discretized domain, with $\boldsymbol{Q}^{(q)}$ and $\boldsymbol{Q}^{(q)^T}$ being the kinematic and static incidence matrices, respectively, $\boldsymbol{R}$ is the global resultant force vector, and $\overline{\boldsymbol{u}}$ is the global surface-averaged displacement vector.

The modified global stiffness matrix allows the adoption of energetically conjugated quantities, i.e., the surface-averaged displacements and the resultant forces acting on the subvolume faces. This adjustment not only guarantees better physical consistency but also improves computational efficiency by enabling the use of solvers optimized for symmetric systems. As a result, the time required to solve the modified global system of equations is significantly reduced, bringing the computational cost closer to the finite element method-based approaches while retaining the benefits of the finite-volume theory in terms of numerical stability and checkerboard-free solutions.

3. Topology optimization problems for compliance minimization

A significant portion of the progress in topology optimization has been made through the consideration of compliance minimization problems, whose concepts are well-established in the context of finite-element strategies. In this study, we implement the compliance minimization problem using linear elastic stress analysis based on the finite-volume theory. According to Araujo et al. (2021), the total work done by external loadings and the total strain energy of a deformed structure are equal for quasi-static analysis in the context of the standard finite-volume theory. As a result, the nested topology optimization problem for compliance minimization can be written as

$$\begin{cases} \text{Find } \boldsymbol{\rho} \text{ which minimizes } C(\boldsymbol{\rho}) = \sum_{q=1}^{N_q} \overline{\boldsymbol{u}}^{(q)^T} \overline{\boldsymbol{K}}^{(q)^T} \overline{\boldsymbol{u}}^{(q)} = \sum_{q=1}^{N_q} E_q\left(\rho_q\right) \overline{\boldsymbol{u}}^{(q)^T} \overline{\boldsymbol{K}}_0^{(q)^T} \overline{\boldsymbol{u}}^{(q)} \\ \qquad\qquad \text{subject to:} \\ \qquad\qquad \dfrac{V(\boldsymbol{\rho})}{\overline{V}} = f \\ \qquad\qquad 0 \le \rho_q \le 1 \end{cases}, \tag{8}$$

where $C(\boldsymbol{\rho})$ is the compliance function, defined as twice the work done by external loadings, $\boldsymbol{\rho}$ is the relative density vector, ρ_q is the relative density associated with the subvolume q, $\overline{\boldsymbol{K}}_0^{(q)}$ is the subvolume modified stiffness matrix for a subvolume with unit Young's modulus, f is the volume fraction, and $V(\boldsymbol{\rho})$ and $\overline{V}$ are the material and reference domain volumes, respectively.

The problem presented in Eq. (8) is solved with a nested iterative loop, where at each iteration, the displacement $\overline{\boldsymbol{u}}$ is computed by solving the modified global system of equations presented in Eq. (7). The two major material interpolation functions are implemented in the algorithm: SIMP (Sigmund, 2007) and RAMP (Stolpe and Svanberg, 2001). The Young's modulus $E_q(\rho_q)$ of each subvolume can be evaluated by the following expressions:

$$E_q\left(\rho_q\right) = E_{min} + \rho_q^p (E_0 - E_{min}) \text{ for SIMP}$$
$$E_q\left(\rho_q\right) = E_{min} + \frac{\rho_q}{1 + a\left(1 - \rho_q\right)}(E_0 - E_{min}) \text{ for RAMP} , \tag{9}$$

where p and a are the penalization factors for SIMP and RAMP methods, respectively, E_0 is the material stiffness, and E_{min} is the soft (void) material stiffness, which is a non-zero positive low value to avoid the singularity in the stiffness matrix. Figure 3 shows the concavity of the penalization functions performed by the SIMP and RAMP methods as presented by Eq. (9), where the ratio E_{min}/E_0 is adopted as 10^{-9}. The RAMP method presents a more gradual increase in its concavity when compared to the SIMP method, which softens the numerical response of this method. The function concavity observed in the RAMP method is smoother and presents a slower convergence to the limit relative density values (0 or 1), as observed in the green (RAMP for $a = 1$) and blue (RAMP for $a = 2$) lines, which incurs in a more gradual convergence for this method. On the other hand, the SIMP method concentrates the relative density values in 0 or 1, as observed in concavity of the orange (SIMP for $p = 2$) and yellow (SIMP for $p = 3$) lines, promoting a faster convergence to the black and white design.
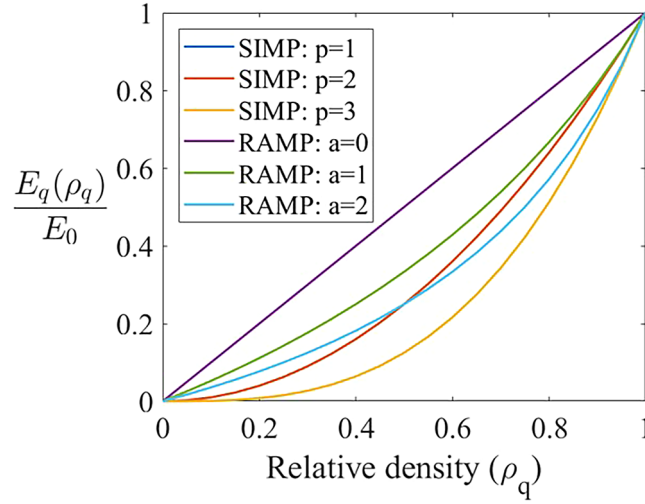
Figure 3. SIMP and RAMP methods' penalization functions.

3.1 Objective function gradient

The gradient of the compliance with respect to the subvolume density ρ_r can be determined by

$$\frac{\partial C(\boldsymbol{\rho})}{\partial \rho_r} = \sum_{q=1}^{N_q} \left[\frac{\partial \overline{\boldsymbol{u}}^{(q)T}}{\partial \rho_r} \overline{\boldsymbol{K}}^{(q)T} \overline{\boldsymbol{u}}^{(q)} + \overline{\boldsymbol{u}}^{(q)T} \frac{\partial \overline{\boldsymbol{K}}^{(q)T}}{\partial \rho_r} \overline{\boldsymbol{u}}^{(q)} + \overline{\boldsymbol{u}}^{(q)T} \overline{\boldsymbol{K}}^{(q)T} \frac{\partial \overline{\boldsymbol{u}}^{(q)}}{\partial \rho_r} \right]. \tag{10}$$

Employing $\overline{\boldsymbol{K}}^{(q)T} = \overline{\boldsymbol{K}}^{(q)}$, the Eq. (10) can be simplified to

$$\frac{\partial C(\boldsymbol{\rho})}{\partial \rho_r} = \overline{\boldsymbol{u}}^{(r)T} \frac{\partial \overline{\boldsymbol{K}}^{(r)}}{\partial \rho_r} \overline{\boldsymbol{u}}^{(r)} + 2 \sum_{q=1}^{N_q} \left[\overline{\boldsymbol{u}}^{(q)T} \overline{\boldsymbol{K}}^{(q)} \frac{\partial \overline{\boldsymbol{u}}^{(q)}}{\partial \rho_r} \right]. \tag{11}$$

The Eq. (11) can be rewritten as

$$\frac{\partial C(\boldsymbol{\rho})}{\partial \rho_r} = \overline{\boldsymbol{u}}^{(r)T} \frac{\partial \overline{\boldsymbol{K}}^{(r)}}{\partial \rho_r} \overline{\boldsymbol{u}}^{(r)} + 2\overline{\boldsymbol{u}}^T \overline{\boldsymbol{K}} \frac{\partial \overline{\boldsymbol{u}}}{\partial \rho_r} = \overline{\boldsymbol{u}}^{(r)T} \frac{\partial \overline{\boldsymbol{K}}^{(r)}}{\partial \rho_r} \overline{\boldsymbol{u}}^{(r)} + 2\boldsymbol{R}_p^T \frac{\partial \overline{\boldsymbol{u}}_u}{\partial \rho_r} + 2\boldsymbol{R}_u^T \frac{\partial \overline{\boldsymbol{u}}_p}{\partial \rho_r}, \tag{12}$$

where $\boldsymbol{R}_p$ and $\overline{\boldsymbol{u}}_p$ are the prescribed force and displacement vectors, respectively, and $\boldsymbol{R}_u$ and $\overline{\boldsymbol{u}}_u$ are the unknown force and displacement vectors, respectively. In terms of these vectors, the global system of equations can be decomposed as follows

$$\begin{bmatrix} \boldsymbol{R}_p \\ \boldsymbol{R}_u \end{bmatrix} = \begin{bmatrix} \overline{\boldsymbol{K}}_{pu} & \overline{\boldsymbol{K}}_{pp} \\ \overline{\boldsymbol{K}}_{uu} & \overline{\boldsymbol{K}}_{up} \end{bmatrix} \begin{bmatrix} \overline{\boldsymbol{u}}_u \\ \overline{\boldsymbol{u}}_p \end{bmatrix}. \tag{13}$$

The subscripts in Eq. (13) reflect the relationship between prescribed and unknown quantities, where the first index refers to forces and the second to displacements. The letter "u" denotes unknown quantities, while "p" represents prescribed ones. Therefore, the submatrix $\overline{K}_{pu}$ expresses the coupling between prescribed forces and unknown displacements, while $\overline{K}_{pp}$ defines the relationship between prescribed forces and prescribed displacements. Similarly, $\overline{K}_{up}$ describes the interaction between unknown forces and prescribed displacements, and $\overline{K}_{uu}$ corresponds to the relationship between unknown forces and unknown displacements. This indexing scheme distinguishes between the interactions of prescribed and unknown quantities within the stiffness matrix.

Once $\partial \overline{\boldsymbol{u}}_p / \partial \rho_r = \boldsymbol{0}$, the Eq. (12) can be simplified to

$$\frac{\partial C(\boldsymbol{\rho})}{\partial \rho_r} = \overline{\boldsymbol{u}}^{(r)T} \frac{\partial \overline{\boldsymbol{K}}^{(r)}}{\partial \rho_r} \overline{\boldsymbol{u}}^{(r)} + 2\boldsymbol{R}_p^T \frac{\partial \overline{\boldsymbol{u}}_u}{\partial \rho_r}. \tag{14}$$

Thus, there are two cases, as described below.

Case 1: prescribed displacement ($\boldsymbol{R}_p = \boldsymbol{0}$ and $\overline{\boldsymbol{u}}_p \neq \boldsymbol{0}$), which implies in the maximization of $C(\boldsymbol{\rho})$.

$$\frac{\partial C(\boldsymbol{\rho})}{\partial \rho_r} = \overline{\boldsymbol{u}}^{(r)T} \frac{\partial \overline{\boldsymbol{K}}^{(r)}}{\partial \rho_r} \overline{\boldsymbol{u}}^{(r)} \tag{15}$$

Case 2: prescribed force ($\boldsymbol{R}_p \neq \boldsymbol{0}$ and $\overline{\boldsymbol{u}}_p = \boldsymbol{0}$), which implies in the minimization of $C(\boldsymbol{\rho})$.

$$\frac{\partial C(\boldsymbol{\rho})}{\partial \rho_r} = \overline{\boldsymbol{u}}^{(r)T} \frac{\partial \overline{\boldsymbol{K}}^{(r)}}{\partial \rho_r} \overline{\boldsymbol{u}}^{(r)} + 2\overline{\boldsymbol{u}}_u^T \overline{\boldsymbol{K}}_{pu} \frac{\partial \overline{\boldsymbol{u}}_u}{\partial \rho_r} \tag{16}$$

Differentiating $\boldsymbol{R}_p = \overline{\boldsymbol{K}}_{pu}\overline{\boldsymbol{u}}_u$ in relation to ρ_r, follows

$$\boldsymbol{0} = \frac{\partial \overline{\boldsymbol{K}}_{pu}}{\partial \rho_r} \overline{\boldsymbol{u}}_u + \overline{\boldsymbol{K}}_{pu} \frac{\partial \overline{\boldsymbol{u}}_u}{\partial \rho_r} \quad \therefore \quad \overline{\boldsymbol{K}}_{pu} \frac{\partial \overline{\boldsymbol{u}}_u}{\partial \rho_r} = -\frac{\partial \overline{\boldsymbol{K}}_{pu}}{\partial \rho_r} \overline{\boldsymbol{u}}_u. \tag{17}$$

Thus

$$\frac{\partial C(\boldsymbol{\rho})}{\partial \rho_r} = \overline{\boldsymbol{u}}^{(r)T} \frac{\partial \overline{\boldsymbol{K}}^{(r)}}{\partial \rho_r} \overline{\boldsymbol{u}}^{(r)} - 2\overline{\boldsymbol{u}}_u^T \frac{\partial \overline{\boldsymbol{K}}_{pu}}{\partial \rho_r} \overline{\boldsymbol{u}}_u. \tag{18}$$

Considering $\overline{\boldsymbol{u}}_p = \boldsymbol{0}$, follows

$$\overline{\boldsymbol{u}}_u^T \frac{\partial \overline{\boldsymbol{K}}_{pu}}{\partial \rho_r} \overline{\boldsymbol{u}}_u = \overline{\boldsymbol{u}}^T \frac{\partial \overline{\boldsymbol{K}}}{\partial \rho_r} \overline{\boldsymbol{u}} = \overline{\boldsymbol{u}}^{(r)T} \frac{\partial \overline{\boldsymbol{K}}^{(r)}}{\partial \rho_r} \overline{\boldsymbol{u}}^{(r)}. \tag{19}$$

This implies

$$\frac{\partial C(\boldsymbol{\rho})}{\partial \rho_r} = \overline{\boldsymbol{u}}^{(r)T} \frac{\partial \overline{\boldsymbol{K}}^{(r)}}{\partial \rho_r} \overline{\boldsymbol{u}}^{(r)} - 2\overline{\boldsymbol{u}}^{(r)T} \frac{\partial \overline{\boldsymbol{K}}^{(r)}}{\partial \rho_r} \overline{\boldsymbol{u}}^{(r)} = -\overline{\boldsymbol{u}}^{(r)T} \frac{\partial \overline{\boldsymbol{K}}^{(r)}}{\partial \rho_r} \overline{\boldsymbol{u}}^{(r)}, \tag{20}$$

which results in

$$\frac{\partial C(\boldsymbol{\rho})}{\partial \rho_r} = -\frac{dE_r(\rho_r)}{d\rho_r} \overline{\boldsymbol{u}}^{(r)T} \overline{\boldsymbol{K}}_0^{(r)} \overline{\boldsymbol{u}}^{(r)}, \tag{21}$$

where

$$\begin{aligned} \frac{dE_r(\rho_r)}{d\rho_r} &= p\rho_r^{p-1}(E_0 - E_{min}) \text{ for SIMP} \\ \frac{dE_r(\rho_r)}{d\rho_r} &= \frac{1+a}{[1+a(1-\rho_r)]^2}(E_0 - E_{min}) \text{ for RAMP.} \end{aligned} \tag{22}$$

The examples analyzed in the following sections are associated with the second case, where a prescribed force is applied, and all the prescribed displacements are zero.

3.2 Optimality criteria method
The proposed optimization problem is solved employing the OC method. Following Sigmund (2001) and Andreassen et al. (2011), a heuristic updating scheme identical to the scheme proposed in Bendsøe (1995) can be employed as

$$\rho_q^{new} = \begin{cases} \max\left(0, \rho_q - m\right), & \text{if } \rho_q B_q^\eta \leq \max\left(0, \rho_q - m\right), \\ \min\left(1, \rho_q + m\right), & \text{if } \rho_q B_q^\eta \geq \min\left(1, \rho_q + m\right), \\ \rho_q B_q^\eta, & \text{otherwise} \end{cases} \tag{23}$$

where m is a positive move-limit, η is a numerical damping factor, and B_q is the optimality condition defined as

$$B_q = \frac{-\frac{\partial C}{\partial \rho_q}}{\lambda \frac{\partial V}{\partial \rho_q}}, \qquad (24)$$

where the Lagrange multiplier λ can be found by means of a bisection algorithm.

The damping factor can be employed to regularize possible oscillations during the optimization, mainly when no filtering techniques are employed. The parameter η is directly related to the method performance, once this affects the speed variation of B_q^η (Montes, 2016). A high value for η can accelerate the optimization convergence process, which may cause oscillations in the displacement field for the low-density regions (Ma et al., 1993). Also, the adoption of minor values of η can prevent divergence in the topology optimization algorithm; however, this results in small changes in the design variables, which leads to a slower convergence process (Ma et al., 1993). The value of η that provides the faster convergence for the overall process is 1/2, so it is recommended to maintain the damping factor as close as possible of this value.

3.3 Mesh-independent filters

As discussed by Araujo et al. (2020b), the topology optimization problem based on the finite-volume theory is a checkerboard-free approach; however, it is observed the occurrence of the mesh-dependency numerical issue. As a result, for topology problems employing the finite-volume theory, filtering techniques are employed to circumvent the mesh dependence issue. Filtering techniques intend to regularize topology optimization numerical issues by using density or sensitivity-based methods. For the density-based methods, each subvolume is redefined by a weighted average of the densities in the subvolume neighborhood, which modifies the sensitivities after the finite-volume analysis. For the strategy based on sensitivity methods, the finite-volume theory analysis is performed, and the sensitivities are consistently calculated; subsequently, they are heuristically recalculated by weighted averaged functions of the sensitivities in the neighboring subvolumes (Sigmund, 2007).

For the sensitivity-based strategy, the employed filtering technique modifies the subvolumes' sensitivities as follows

$$\frac{\partial C}{\partial \rho_q} = \frac{1}{\max\left(\gamma, \rho_q\right) \sum_{i \in N} \widehat{H}_{qi}} \sum_{i \in N} \widehat{H}_{qi} \rho_i \frac{\partial C}{\partial \rho_i}, \qquad (25)$$

where $\gamma = 10^{-3}$ is a small positive real value introduced to avoid division by zero, N is the set of subvolumes i for which the center-to-center distance $\Delta(q,i)$ to subvolume q is smaller than the filter radius r_{min}, and $\widehat{H}_{qi}$ is a weight factor evaluated as (Andreassen et al., 2011)

$$\widehat{H}_{qi} = \max\left(0, r_{min} - \Delta(q,i)\right), \qquad (26)$$

The density filter modifies, besides the sensitivities, the original densities ρ_q as follows

$$\widehat{\rho}_q = \frac{1}{\sum_{i \in N} \widehat{H}_{qi}} \sum_{i \in N} \widehat{H}_{qi} \rho_i, \qquad (27)$$

where $\widehat{\rho}_q$ are referred to as the physical densities, as the application of a density filter causes the original densities ρ_q to lose their physical meaning (Sigmund, 2007). When the density filter is employed, the objective function sensitivities with respect to the physical densities $\widehat{\rho}_q$ are given by Eq. (21) once the design variables ρ_q are replaced by $\widehat{\rho}_q$.

4. Software description

Top2DFVT is an algorithm developed to obtain optimized topologies using the finite-volume theory for linear elastic continuum structures. The first use of this algorithm performed by Araujo et al. (2020a) was based on the implementation suggested by the top99 code (Sigmund, 2001), where some operations, such as the filtering procedure and matrices assembly, dramatically increase the computational cost. Therefore, the main features of the top88 code are now explored in this version, such as loop vectorization and memory preallocation, which are strengths of Matlab explored in this program. Additionally, some parts of the code are moved out of the optimization loop, guaranteeing they are only performed once. From the top99neo code, the **fsparse** function is implemented for finite-volume theory matrices assembly, which guarantees a gain of computational efficiency by accelerating the preallocation of these large matrices. The program also explores two new advances in the OC method promoted by the top99neo code. The first advancement incorporates a better approximation for the initial guess of the interval of the Lagrange multiplier λ in the bisection method. This improvement reduces the number of iterations operated by the OC method by suggesting initial values closer to the final solution in the iterative process of the bisection method. The second advancement involves avoiding the application
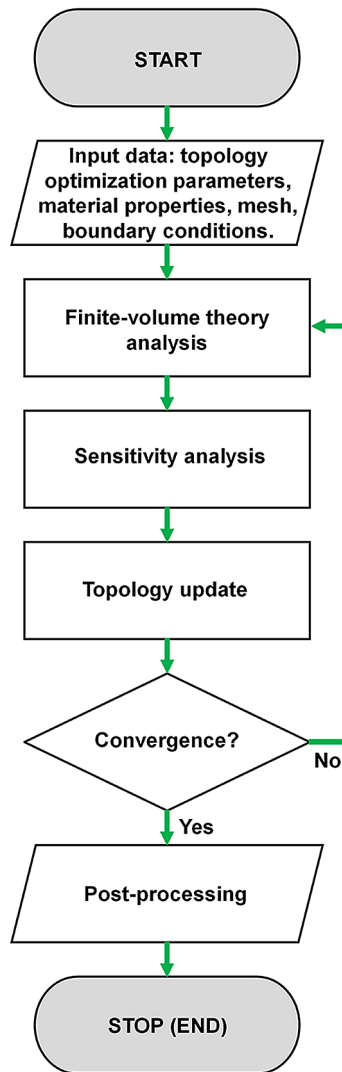
START

Input data: topology optimization parameters, material properties, mesh, boundary conditions.

Finite-volume theory analysis

Sensitivity analysis

Topology update

Convergence?

No

Yes

Post-processing

STOP (END)

Figure 4. Flowchart of the Top2DFVT for the topology optimization of linear elastic continuum structures.

of a filter at each bisection step when checking the volume constraint with the physical field. This alternative reduces the processing time of each bisection iteration and represents another improvement inspired by the top99neo code.

The proposed algorithm is a collection of Matlab functions written in 175 lines, disregarding the commented lines, that implement the design domain, material properties, finite-volume theory analysis, topology optimization, mesh-independency filters, and post-processing, as shown in the flowchart in Figure 4. In the data initialization step, the design domain and material properties are defined as inputs to the topology optimization problem, and homogeneous rectangular subvolumes are adopted in the discretized domain. The relative density of each subvolume in the discretized domain is taken as constant. The finite-volume theory analysis is performed for structured meshes considering linear elastic materials for plane stress state. The gradient-based topology optimization problem for compliance minimization is solved employing the OC method, considering a move limit of 0.2. The stopping criterium is set up as follows: 1% of tolerance for the maximum change in the design variables between successive steps. Two mesh-independent filters are implemented: a sensitivity filter and a density filter based on the filtering approaches presented by Andreassen et al. (2011). Finally, the algorithm prints the obtained optimized topology and the investigated numerical aspects, such as the number of iterations, processing time, compliance estimations, etcetera.

In the Top2DFVT implementation, memory preallocation is crucial in enhancing computational efficiency by reducing the time required for matrix assembly and solving linear systems. However, this performance gain comes at the expense of increased memory usage, as large data structures must be allocated in advance. This trade-off between computational
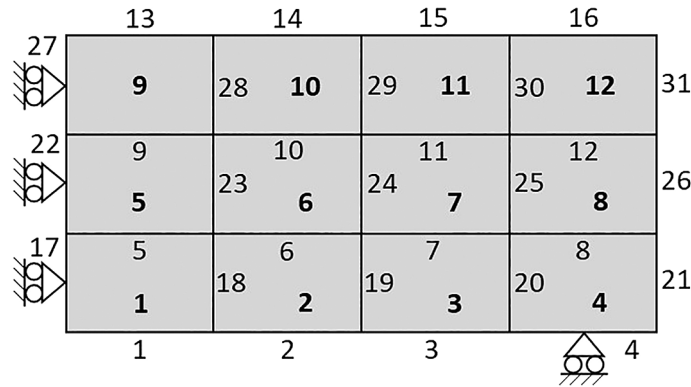
Figure 5. Analysis domain with 12 subvolumes and face indexing.

speed and memory consumption is a common consideration in the design of topology optimization algorithms. While the memory overhead is manageable for medium-sized problems, it can become significant for large-scale applications. Therefore, careful management of memory resources is essential to balance efficiency and scalability.

4.1 Software architecture

The algorithm is initialized by entering the following line in the Matlab command prompt:

```
Top2DFVT(L,H,nx,ny,volfrac,penal,frad,ft,varargin)
```

where L and H indicate the horizontal and vertical analysis domain length, respectively, nx and ny are the number of subvolumes in the horizontal and vertical directions, respectively, volfrac is the prescribed volume fraction constraint, penal is the penalty factor, frad is the filter radius, ft specifies whether sensitivity filter (ft = 1), or density filter (ft = 2), or no filter (ft = 0), and varargin activates the use of the *fsparse* routine when set up as 'fast'. In Top2DFVT.m file, the major sections are default parameters' declaration, initialization of design variables, domain initialization, local stiffness matrix calculation, material interpolation, filtering initialization, topology optimization iterative process, and post-processing.

The default parameters indicate the value of the applied concentrated load, the material Young's modulus, the soft material stiffness, the Poisson ratio, the type of penalization method, the damping factor, and the maximum number of iterations. Fundamentally, the soft material stiffness must be a minimal value larger than zero, and the type of penalization method can be chosen between 'SIMP' or 'RAMP' for the material interpolation scheme. While the initialization of the design variables step establishes the discretization of the analysis domain by indexing each subvolume, allocating the relative density, and the volume-constrained gradient matrix. Therefore, the design domain is assumed to be rectangular and discretized in rectangular subvolumes. An example of a coarse mesh composed of 12 subvolumes with four edges per subvolume and two degrees of freedom (DOFs) per face is shown in Figure 5.

The subvolume is indexed row-wise from left to right and down to up, as represented by the bold number shown in Figure 5. Similarly, the subvolume faces are numbered from left to right and down to up, however, the horizontal faces are first indexed, followed by the indexing of the vertical faces, as illustrated in Figure 5. As a result, two DOFs are defined in each subvolume face, where the DOFs $2j - 1$ and $2j$ correspond to the horizontal and vertical displacement of face j, respectively. The DOFs assemblage is operated by the subroutine:

```
[dof,ndof,ijK] = DOFassembly(nx,ny)
```

where dof is the matrix containing the subvolume DOFs, ndof is the total number of DOFs, and ijK is the indexing matrix employed for the global stiffness matrix assemblage.

The row iK and column jK index vectors are generated by a Kronecker matrix product with a unit vector of 8 lines. The resulting vectors iK and jK are structured so that the iK(i) and jK(j) indices correspond to the assemblage of the stiffness matrix for the subvolume q. The assembly of the global system of equations is performed by employing the *sparse* function in Matlab, which takes three vectors as input arguments: the first and second contain the row and column indices of the non-zero entries, while the third vector contains the entry values of the sparse vectors and matrices. It can be also suggested the use of the *fsparse* routine, developed by Engblom and Lukarski (2016), which enhances the sparse

assembly by providing a better ordering of the performed operations. Although Ferrari and Sigmund (2020) have achieved a speedup of 170-250% in the algorithm compared to sparse function on a single-core processor, the performance achieved in our computational environment is similar for both routines. The *fsparse* routine is performed by setting the variable varargin as 'fast', while the absence of values for this variable indicates the use of the 'sparse' routine.

The structure supporting conditions are prescribed in supp vector by specifying which DOFs of the discretized domain are fixed, while the natural boundary conditions are specified directly in the global force vector F by addressing the DOFs with prescribed loads and their respective magnitude force values. The assemblage of the global stiffness matrix is operated by the function

```
K = StiffnessAssemblage(sK)
```

for sK = K0(:)*E(:)', where K0 is the local stiffness matrix for a unitary elastic modulus obtained with the function

```
K0 = LocalStiffMatrix(nu,l,h)
```

and E is the chosen material interpolation scheme. While the local stiffness matrix is symmetric, rounding errors during the assembly of the global stiffness matrix using the *sparse* or *fsparse* commands can cause asymmetry. To correct this, symmetry is enforced at the global level, improving the efficiency of the Matlab backslash (\) command, as recommended by Andreassen et al. (2011).

After solving the global system of equations, the subvolume compliance and its sensitivities are calculated. The objective function value is obtained by adding the individual contribution of each subvolume in the discretized domain, while the subvolume sensitivities are modified considering the aspects of the chosen filtering technique. Subsequently, the design variables are updated by the OC method. The convergence criterium is adopted as 1% of tolerance for the maximum change in design variables. As post-processing step, the investigated numerical aspects are printed, followed by the plotting of the optimized topology. Finally, the processing time is computed for the performed analysis.

5. Illustrative examples

The performed example is a cantilever deep beam subject to a concentrated load, as shown in Figure 6. In this case, the vertical and horizontal averaged displacements at the edges of the left border of the structure are fixed, so the supp vector is set up as

```
supp = unique (dof(1:nx:end-nx+1,7:8))
```

and the concentrated load is positioned in the middle of the right border in the structure, therefore, the global force vector F is given by

```
F = sparse (dof (nx*(ny+1)/2,4)',1,P,ndof,1)
```

In this example, the dimensions of the cantilever deep beam are $L = 100$ and $H = 50$, and the concentrated load is applied at the center of the free edge. To ensure the load is applied to the face of a single subvolume, the number of subvolumes in
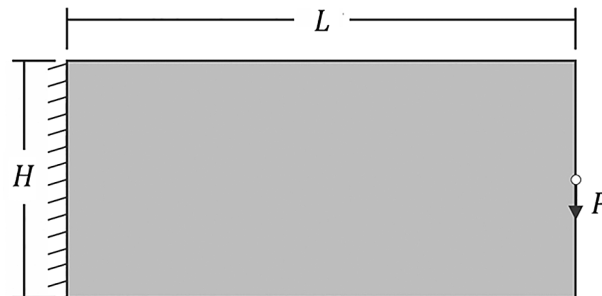

Figure 6. Cantilever deep beam.

the vertical direction must be odd. Furthermore, to generate an analysis domain with square subvolumes, the number of subvolumes in the horizontal direction must be twice the number of those in the vertical direction.

The data initialization is set up as $P = -1$, for the applied concentrated load, $E_0 = 1$, for the Young's modulus, $E_{min} = 10^{-9}$, for the soft material stiffness, $v = 0.3$, for the Poisson's ratio, $\eta = 1/2$, for the damping factor, $move = 0.2$, for the move-limit, and $maxit = 100$, for the maximum number of iterations. For the approaches using the SIMP model, the damping factor is adjusted to 1/2.6 to avoid the oscillatory phenomenon, as discussed by Araujo et al. (2020a,b). The computational environment in terms of programming language and machine can be defined as Matlab R2023a (64-bits) for Windows 11, accompanied by the Optimization and Parallel Computing toolboxes, and processor of 12th Gen Intel(R) Core (TM) i7-1260P 2.10 GHz, RAM 16.0 GB DDR5.

Considering the same parameters employed by Araujo et al. (2020a) in the filtering scenario, the algorithm can be started by the following command:

```
Top2DFVT(100,50,202,101,0.4,1:0.5:4,0.71,1)
```

which consists in the application of the sensitivity filter considering the adjacent subvolumes with a filter radius of 0.71, given by approximately $1.01\sqrt{l_q^2 + h_q^2}$, where l_q and h_q represent the subvolume dimensions, and a volume fraction of 40% of the total volume. The *fsparse* routine can be performed by including varargin = 'fast' in the Top2DFVT command. The obtained optimized topologies for the SIMP model are shown in Figure 7, where Figure 7a, 7b, and 7c show the optimized topologies obtained by employing the sensitivity, density, and no filtering techniques, respectively. The investigated numerical aspects are presented in Table 1. In general, the obtained optimized topologies have shown to be checkerboard-free and the employed filtering techniques have qualitatively reduced the mesh dependency issue. Araujo et al. (2020a,b) have already verified these features; however, the current algorithm has obtained similar results by reducing the computational cost by 99.8%. For instance, the same analysis performed for a cantilever deep beam using the sensitivity filter with a mesh of 20,402 subvolumes took 10 hours, 28 minutes, and 37 seconds in Araujo et al. (2020a), while the same analysis employing the Top2DFVT algorithm took only 1 minute and 6 seconds, as shown in Table 1.

For the RAMP approach, the penalty factor variable is adjusted to penal = 0:0.5:3, and the variable model is modified to 'RAMP'. The optimized topologies obtained for the RAMP model are shown in Figure 8, considering the application of the sensitivity filter, Figure 8a, density filter, Figure 8b, and no filtering, Figure 8c. In general, they are checkerboard-free optimized topologies with a reduction in the obtained structural compliance values compared to the optimized topologies generated by the SIMP model, as presented in Table 1. The no-filter approach generated an optimized structure like the optimized topologies obtained by employing the SIMP model and mesh-independent filters. Thus, the RAMP model coupled with the finite-volume theory has shown to be checkerboard-free and mesh-independent for the cantilever
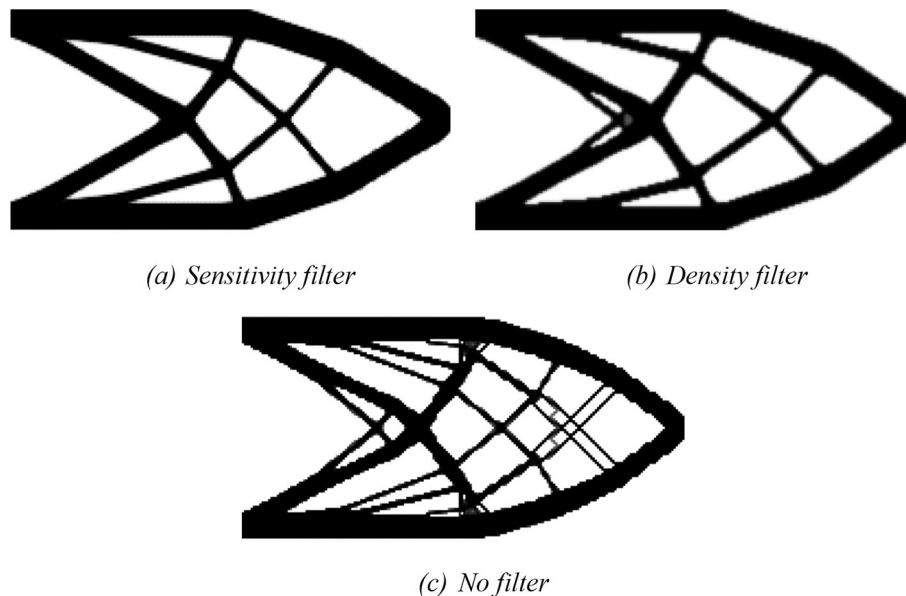

(a) Sensitivity filter

(b) Density filter

(c) No filter

Figure 7. Optimized topologies for the cantilever deep beam employing the SIMP material interpolation.

Table 1. Investigated numerical aspects of the cantilever deep beam with a discretization of 20,402 subvolumes.

SIMP method			
Analysis	**Sensitivity filter**	**Density filter**	**No filter**
Compliance (J)	88.12	91.02	87.90
Filter radius	0.71	0.71	0
Number of iterations	368	577	391
Processing time (*sparse*)	1min 6s	1min 58s	1min 3s
Processing time (*fsparse*)	1min 5s	1min 38s	1min 10s
RAMP method			
Analysis	**Sensitivity filter**	**Density filter**	**No filter**
Compliance (J)	85.86	87.69	84.49
Filter radius	0.71	0.71	0
Number of iterations	397	614	451
Processing time (*sparse*)	1min 1s	1min 38s	1min 16s
Processing time (*fsparse*)	1min 3s	1min 41s	1min 13s

(a) Sensitivity filter

(b) Density filter

(c) No filter
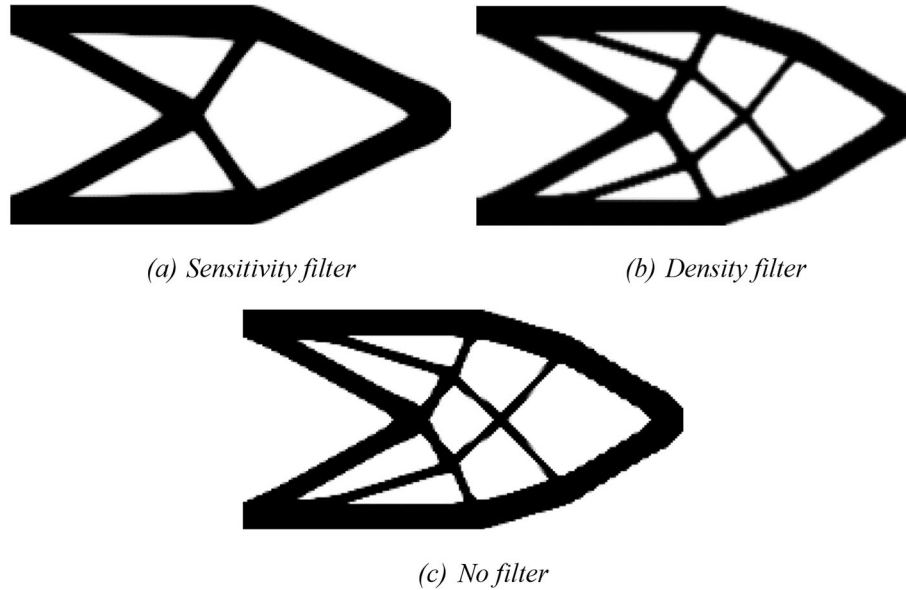
Figure 8. Optimized topologies for the cantilever deep beam employing the RAMP material interpolation.

deep beam example, which are desired features for manufacturing purposes. In addition, the sensitivity filter for RAMP model has obtained better results by reducing the optimized structural perimeter even more. Table 1 also presents the investigated numerical aspects for the cantilever deep beam example considering the RAMP model. The approach based on the sensitivity filter has presented the lowest number of iterations and computational cost, while the density filter has shown the highest processing time. The minimum value for structural compliance is observed when the no-filtering technique is employed.

Adopting the continued penalization scheme, combined with a highly restrictive local convergence criterion, increases the number of iterations in the investigated examples, especially for the most refined meshes, where achieving local convergence is more challenging. The smooth local response produced by the sensitivity filter accelerates convergence compared to the optimization process without filtering techniques, a result not observed with the density filter. Figure 9 displays the objective function histories throughout the optimization process of the cantilever deep beam for the SIMP
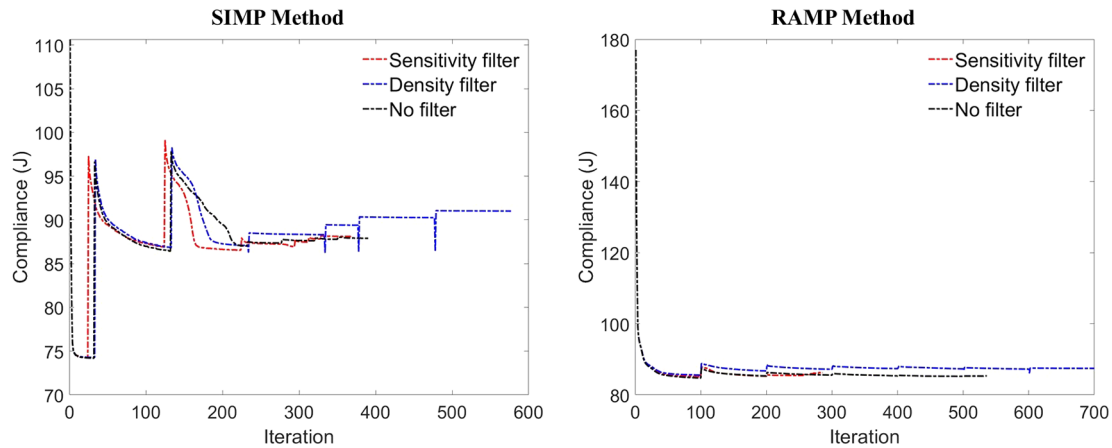
Figure 9. Objective function histories for the SIMP and RAMP methods.

and RAMP methods, highlighting that the density filter demands more iterations for convergence. In contrast, the optimization process with the sensitivity filter achieves the fastest convergence. The RAMP method provides closer values for the objective function throughout the optimization process for the three approaches adopted: results without filters, with the sensitivity filter, and with the density filter. Furthermore, the RAMP method demonstrates a more stable convergence process than the SIMP method for these approaches. Notably, the jumps in the continued penalization scheme are significantly smaller for the RAMP method than those between different penalty factors in the SIMP method.

For computational efficiency, the *fsparse* routine is also implemented; however, for the performed analyses, such a difference in computational cost does not justify using the *fsparse* routine. However, a gain in computational performance is observed by around 30% when meshes with size between 10^5 and 10^6 subvolumes are employed. From Table 1, the non-filtering approach has obtained the optimized topologies with the minimum compliance. In contrast, the density filter approach has obtained the optimized topologies with the maximum values for compliance. In general, Top2DFVT provides a platform to perform 2D topology optimization of structures in Matlab, starting from a domain initialization for structured meshes to data post-processing. Several computational tools have been proposed for topology optimization employing analysis domains discretized with essential features for finite-element approaches. As previously discussed, the finite-volume theory is an alternative technique to the finite-element method in the context of topology optimization algorithms. In addition, this is the first contribution to offer an algorithm that shows the implementation of standard finite-volume theory for structured meshes problems in Matlab. This investigation employs the finite-volume theory in topology optimization for compliance minimization problems.

Top2DFVT offers some advantages, such as:

a) It generates checkerboard-free optimized topologies even when a non-filtering approach is employed.

b) It can be applied to medium and large-scale problems, as the implementation and computational performance are suited to these approaches.

c) It employs different material interpolation methods for topology optimization, such as RAMP and SIMP models. When the non-filtering technique is employed, the optimized topologies generated by the RAMP model usually reduce the perimeter compared to those optimized topologies obtained by the SIMP approach.

The Top2DFVT algorithm is currently being employed for educational and research purposes to promote the advantages of the finite-volume theory in the numerical analysis of structures.

6. Numerical results

In this contribution, three examples are analyzed employing the compliance minimization problem based on the finite-volume theory for linear elastic materials under plane stress state, where the RAMP and SIMP approaches are employed to interpolate the material stiffness. The investigated examples are a cantilever beam subjected to a concentrated load, a Messerschmitt-Bölkow-Blom (MBB) beam, and an L-bracket beam subject to a concentrated load. Some numerical aspects are also investigated during the analyses, such as the number of iterations, processing time, and compliance

estimation. The continued penalization scheme is adopted for the compliance minimization problem, where the penalty factor increases gradually ($\Delta p = 0.25$) from 1 to 4 for SIMP and from 0 to 3 for RAMP. A maximum of 200 iterations is assumed for each performed penalty factor along the optimization process.

6.1 Cantilever deep beam

A classical problem in topology optimization is the cantilever deep beam, whose analysis domain and boundary conditions are illustrated in Figure 10. In this example, it is observed a region of stress concentration where the concentrated load is applied. The adopted geometrical and physical parameters can be described as $H = 450$ mm, $L = 900$ mm, $d = 10$ mm, $P = 1000$ N, $E = 200$ GPa (Young Modulus), and $v = 0.3$ (Poisson's ratio). The proposed optimization problem consists of minimizing the structural compliance, with a volume constraint of 40% of the total volume.

Figure 11 shows the obtained optimized topologies for the approach based on the finite-volume theory considering the SIMP material interpolation method, while Table 2 presents the investigated numerical parameters for each performed analysis. Although the non-filtering approach has obtained the lowest value for the objective function, the sensitivity filter results have presented the lowest computational cost and optimized topologies that better controls the length scale issue, by reducing the formation of thin bars. The density filtering results have shown more thin bars in the optimized topologies when compared to the sensitivity filter, and higher values for the compliance function in the overall investigation. For the SIMP method and considering the non-filtering strategies, the damping factor is adjusted to 1/2.6 to avoid divergence during the optimization process.

The algorithm known as top99neo, proposed by Ferrari and Sigmund in 2020, is used as a benchmark source for the traditional finite-element method for bilinear elements. The algorithm uses the continued penalization scheme, gradually
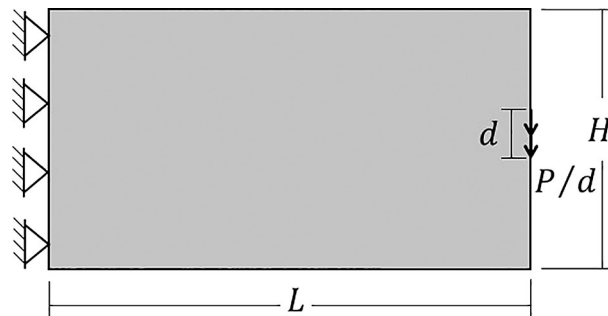

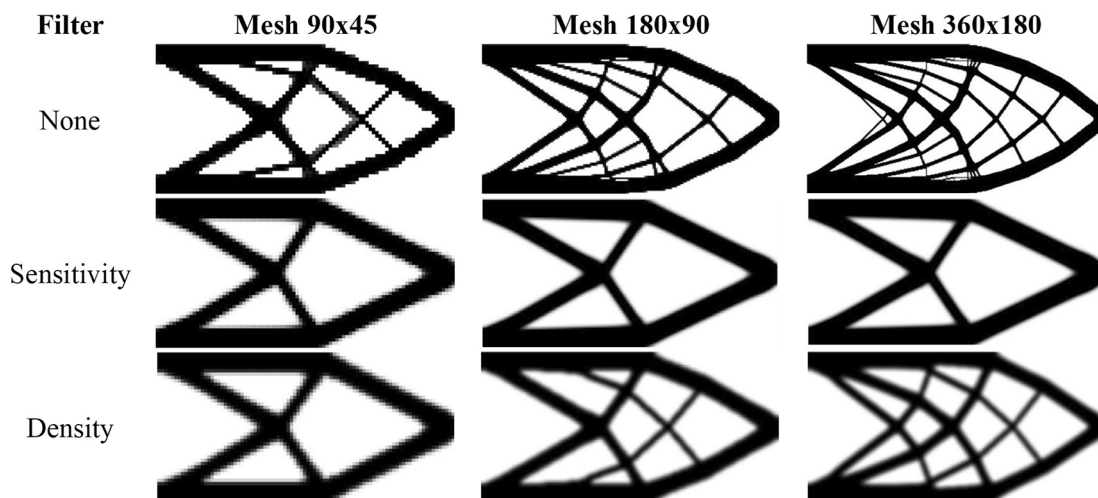**Figure 10. Cantilever deep beam with dimensions and boundary conditions.**

Figure 11. Optimized topologies for the cantilever deep beam obtained by the SIMP approach.

Table 2. Convergence analysis for the cantilever deep beam problem.

SIMP method					
Analysis	**Mesh**	**Number of iterations**	**Processing Time**	**Compliance (J)**	**Filter radius (mm)**
No filter	90x45	371	10s	448.87	0
	180x90	813	4min 11s	391.94	0
	360x180	1183	25min 53s	375.57	0
Sensitivity filter	90x45	213	6s	471.97	15
	180x90	323	1min 25s	406.38	15
	360x180	334	4min 18s	402.01	15
Density filter	90x45	525	15s	491.85	15
	180x90	1450	7min 33s	450.89	15
	360x180	2497	29min 35s	472.49	15
RAMP method					
Analysis	**Mesh**	**Number of iterations**	**Processing Time**	**Compliance (J)**	**Filter radius (mm)**
No filter	90x45	545	15s	435.65	0
	180x90	900	3min 12s	382.82	0
	360x180	1164	24min 26s	369.74	0
Sensitivity filter	90x45	350	9s	453.54	15
	180x90	408	54s	394.17	15
	360x180	465	5min 4s	391.36	15
Density filter	90x45	1010	30s	464.51	15
	180x90	2040	4min 44s	420.37	15
	360x180	2309	47min 10s	419.01	15

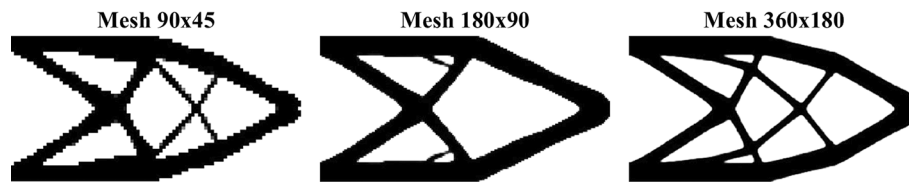Mesh 90x45   Mesh 180x90   Mesh 360x180

Figure 12. Optimized topologies for the cantilever deep beam employing the top99neo algorithm.

increasing the penalty factor ($\Delta p = 0.25$) from 1 to 4, similar to the finite-volume theory approach. Each penalty factor is subjected to 25 iterations. The Heaviside projection parameters are updated throughout the optimization process. The parameter β starts at 2 and increases to 16 by an increment of $\Delta\beta = 2$ every 25 iterations. Figure 12 shows the optimized topologies obtained using the density filter. The filter radius changes to reflect the exact size of the filter radius employed in the finite-volume theory approaches for each mesh size (1.5, 3, and 6, respectively). The optimized topologies obtained using the finite-element approach are more mesh-dependent, even when filtering strategies are employed, as compared to the optimized topologies obtained using the finite-volume theory approach, especially in the case of the results with the sensitivity filter. The computational cost for the finest mesh is 2 minutes and 30 seconds, with a maximum of 350 iterations. The total number of degrees of freedom for the finite-element approach is 132132, while the finite-volume theory approach has a total of 260280 degrees of freedom, which partially explains the difference in computational costs. As the top99neo algorithm employs finite elements with unitary dimensions, it is not feasible to compare the obtained values for the objective function of the optimized topologies.

Figure 13 shows the obtained optimized topologies for the approach based on the RAMP method. In general, the RAMP method has obtained checkerboard-free optimized topologies by reducing the structural perimeter when the non-filtering
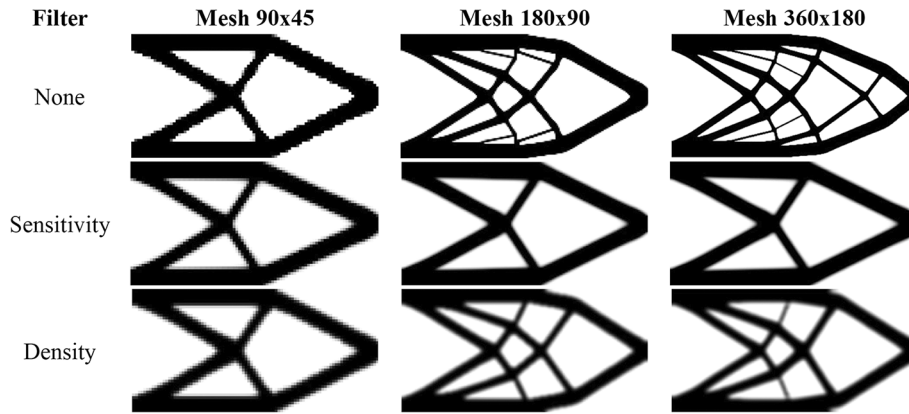
Figure 13. Optimized topologies for the cantilever deep beam obtained by the RAMP approach.

strategy is employed in comparison to the same approach employing the SIMP approach, which is a desired feature for manufacturing purposes. On the other hand, the optimized topologies obtained by the SIMP method usually present a higher structural perimeter by producing more thin bars. Additionally, the RAMP method has obtained a well-defined black-and-white design with lower values for the compliance function, as presented in Table 2.

Table 2 presents the numerical aspects of the performed investigations for the cantilever deep beam example. In general, the RAMP method has presented a higher number of iterations and processing time, although the obtained optimized topologies have presented the lowest values for the objective function. The filter radius is calculated to be slightly higher than $1.01\sqrt{l_q^2 + h_q^2}$ for the coarse mesh. Therefore, the optimized topology obtained for the finest mesh employing the sensitivity filter is very similar to that obtained for the coarse mesh without filtering techniques. This is only possible because the finite-volume theory is a checkerboard-free numerical technique in topology optimization algorithms.

6.2 Half MBB beam

Other classical problem for topology optimization of continuum structures is the Messerschmitt-Bölkow-Blom (MBB) beam. In this case, only half of the structure is analyzed as shown on Figure 14, where the geometric and physical parameters are taken as $H = 300$ mm, $L = 900$ mm, $d = 10$ mm, $P = 1000$ N, $E = 78$ GPa (Young Modulus), and $v = 0.25$ (Poisson's ratio). The volume fraction for the minimum compliance optimization problem is assumed as 40% of the total structure volume.

Figure 15 shows the optimized topologies obtained considering the application of the SIMP method, while Table 3 presents the investigated numerical aspects for each performed analysis. The topology optimization technique considers the non-filtering, sensitivity, and density filtering scenarios. The adopted filter radius is slightly higher than half of the subvolume's diagonal length for the coarsest mesh, which can be written as $1.01\sqrt{l_q^2 + h_q^2}$ and approximated by 15 mm. The no-filter analysis generally generates topologies with more thin bars, while the sensitivity filter obtains cleaner
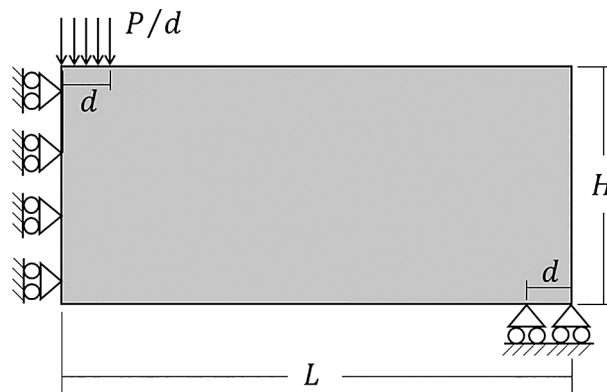

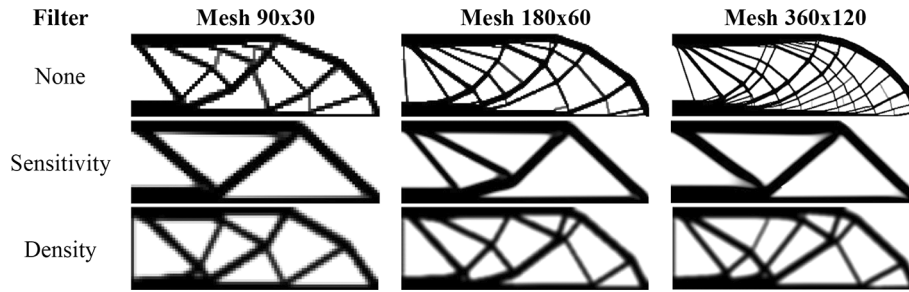**Figure 14. Half-MBB beam with dimensions and boundary conditions.**

Figure 15. Optimized topologies for the MBB beam obtained by the SIMP approach.

Table 3. Convergence analysis for the half MBB beam problem.

SIMP method					
Analysis	**Mesh**	**Number of iterations**	**Processing Time**	**Compliance (J)**	**Filter radius (mm)**
No filter	90x30	538	10s	3160.01	0
	180x60	804	1min 19s	2873.54	0
	360x120	1352	11min 4s	2759.59	0
Sensitivity filter	90x30	410	8s	3174.88	15
	180x60	533	48s	3050.52	15
	360x120	921	7min 26s	2989.76	15
Density filter	90x30	843	15s	3586.61	15
	180x60	1819	4min 59s	3524.15	15
	360x120	2490	20min 51s	3560.40	15
RAMP method					
Analysis	**Mesh**	**Number of iterations**	**Processing Time**	**Compliance (J)**	**Filter radius (mm)**
No filter	90x30	811	15s	2921.81	0
	180x60	1315	2min 50s	2731.09	0
	360x120	1617	17min 14s	2654.87	0
Sensitivity filter	90x30	538	10s	3049.43	15
	180x60	747	1min 51s	2935.32	15
	360x180	1040	8min 27s	2923.79	15
Density filter	90x30	1191	21s	3174.77	15
	180x60	2289	4min 11s	3084.24	15
	360x120	2450	21min 16s	3087.59	15

topologies with a reduced structural perimeter. Besides, the density filter has not presented the same efficiency as the sensitivity filter in reducing the structural perimeter in the final optimized topology, and the obtained compliance is higher when compared to the other approaches. Regarding computational cost, the sensitivity filter approach obtained the lowest processing time and number of iterations, while the density filter approach presented the highest processing time and number of iterations.

Figure 16 shows the optimized topologies obtained employing the top99neo algorithm, where the penalty factor increases gradually ($\Delta p = 0.25$) from 1 to 4 after every 25 iterations until a maximum of 350 iterations, and the beta parameter increases gradually from 2 to 16 ($\Delta \beta = 2$), after every 25 iterations, similarly to the cantilever deep beam example. The optimized topologies shown in Figure 16 are mesh dependents even when filtering strategies are employed. The filter radius is assumed to be 1.5 for the 90×30 mesh, 3 for the 180×60 mesh, and 6 for the 360×120 mesh. When a similar filter radius is employed in the context of the finite-volume theory, this technique demonstrates a less mesh sensitivity
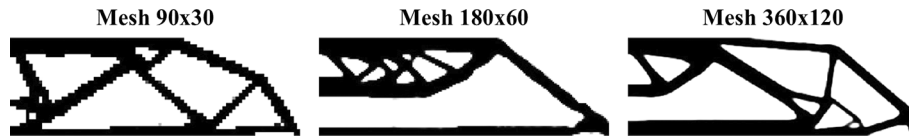
Mesh 90x30　　　　　**Mesh 180x60**　　　　　**Mesh 360x120**

Figure 16. Optimized topologies for the MBB beam employing the top99neo algorithm.

Filter　　**Mesh 90x30**　　　**Mesh 180x60**　　　**Mesh 360x120**
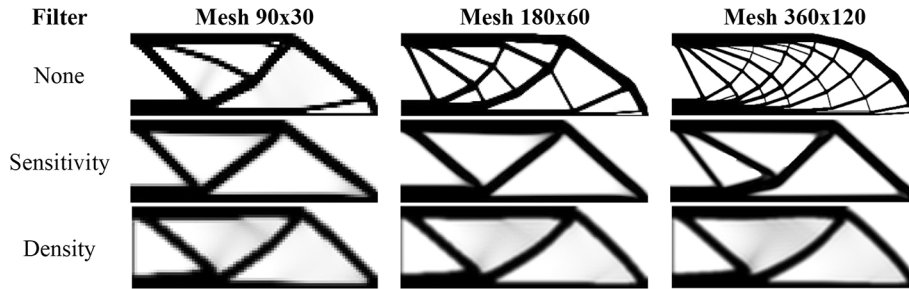
None

Sensitivity

Density

Figure 17. Optimized topologies for the MBB beam obtained by the RAMP approach.

behavior when compared to finite element-based strategies. Regarding computational efficiency, the top99neo code has presented a processing time of 86 seconds for the finest mesh. Generally, the Top2DFVT algorithm presents a higher computational cost when compared to the Q4 finite element-based algorithm. The number of degrees of freedom partially explains this higher computational cost once the total number of degrees of freedom for the finest mesh considering the top99neo algorithm is 87362, while in the Top2DFVT algorithm, the total number of degrees of freedom for the same analysis is 173760. Furthermore, the number of iterations for this example is relatively high for the finite-volume theory approaches once the top99neo algorithm adopts a maximum of 350 iterations.

Figure 17 shows the optimized topologies for the analyses employing the RAMP method, where the adopted filter radius is the same as those employing the SIMP method. The RAMP method has generally obtained optimized topologies with better control of the structural perimeter, even when the non-filtering technique is employed. Additionally, the optimized topology obtained for the coarse mesh without filtering techniques is geometrically close to the optimized topologies for the finest mesh employing filtering strategies. Therefore, the results obtained for the coarse mesh in the no-filter strategy employing the RAMP method could be adopted as the solution for the optimization problem. Table 3 presents the investigated numerical aspects, where the number of iterations and processing time are usually higher for this method when compared to the SIMP approach.

6.3 L-bracket beam

Another analyzed topology optimization problem for stress concentration in two-dimensional structures is the L-bracket beam, whose analysis domain and boundary conditions are illustrated in Figure 18. In the L-bracket beam problem, it is observed a high level of stress concentration in the corner, which is important to check how the new Top2DFVT code leads to these kinds of topology optimization problems. The employed geometric parameters for this beam are assumed as $d = 5$ cm, $L = 100$ cm, and $P = 200$ kN, while the adopted material properties are $E = 70$ GPa (elastic moduli)
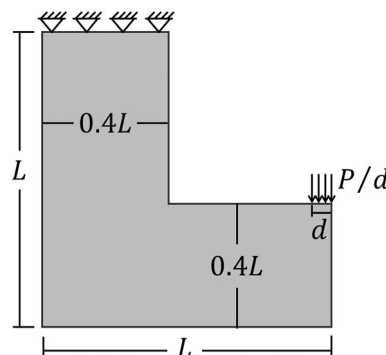

Figure 18. L-bracket beam domain, with d=5 cm, P=200 kN, and L=1 m.
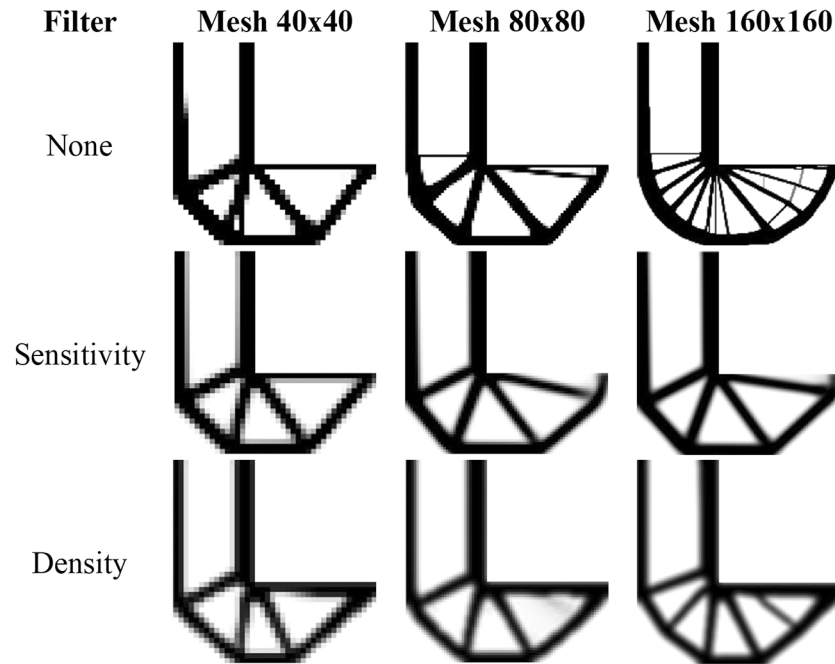
Figure 19. Optimized topologies for the L-bracket beam obtained by the SIMP approach.

and $v = 0.25$ (Poisson's ratio). The proposed optimization problem consists of minimizing the structural compliance function under a volume constraint of 40% of the total volume.

Figure 19 shows the optimized topologies obtained by the SIMP approach for the L-bracket beam problem, considering the absence of filtering techniques and the implementation of the sensitivity and density filters, respectively. The sensitivity filter has reduced the formation of thin bars along the optimized topologies, while the density filter has obtained irregular optimized topologies with the appearance of substantial gray regions. On the other hand, the no-filter strategy has generated well-defined optimized topologies with more thin bars, especially when compared to the sensitivity filter strategy. As Araujo et al. (2020a) suggested, the damping factor is adjusted to 1/2.6 for all performed approaches employing the SIMP to guarantee the absence of the oscillatory phenomenon to any employed filter radius. Table 4 presents the investigated numerical aspects for the performed analyses employing the SIMP method.

The top99neo algorithm is also performed considering the L-bracket beam problem, and the obtained optimized topologies can be observed in Figure 20. As in the previous examples, the same numerical parameters are employed for the physical model, such as the gradual increase in the penalty factor, from 1 to 4 with $\Delta p = 0.25$, and in the Heaviside Projection β parameter, from 2 to 16 with $\Delta \beta = 2$. In terms of computational cost, the top99neo code has presented a processing time of 1 minute and 1 second for the finest mesh, considering a total of 350 iterations, while the Top2DFVT algorithm has presented a processing time of 39 seconds with a total of 155 iterations for of the SIMP method and the sensitivity filter. This difference in processing time can be partially explained by the difference in the total number of iterations observed during the topology optimization analyses. For this example, the Top2DFVT algorithm, considering the sensitivity filter approach, presents a reduced number of iterations for convergence.

Figure 21 presents the obtained optimized topologies by the RAMP method for the L-bracket beam problem. The RAMP method has generally reduced the formation of thin bars, demonstrating less sensitivity with the adopted meshes. As in the SIMP method, the sensitivity filter has shown to be more efficient by reducing the formation of thin bars in the optimized topologies, and the density filter has obtained more irregular topologies with the presence of gray regions. The RAMP method is more stable numerically, and the adopted damping factor is 1/2, which guarantees a faster convergence for the analyses. However, the number of iterations is usually higher for the RAMP method.

Table 4 presents the investigated numerical aspects of the optimized structures, such as the total number of iterations, processing time, and compliance estimation. When the sensitivity filter is employed, there is a remarkable decrease in the number of iterations and computational costs. However, the obtained values for structural compliance are lower when the

Table 4. Convergence analysis for the L-bracket beam problem.

SIMP method					
Analysis	**Mesh**	**Number of iterations**	**Processing Time**	**Compliance (J)**	**Filter radius (cm)**
No filter	40x40	404	4s	4469.64	0
	80x80	698	35s	17388.97	0
	160x160	946	4min 11s	68743.32	0
Sensitivity filter	40x40	274	2s	4794.02	3.6
	80x80	226	10s	19461.58	3.6
	160x160	155	39s	81058.11	3.6
Density filter	40x40	653	6s	6149.43	3.6
	80x80	1140	1min 51s	25552.58	3.6
	160x160	2585	11min 19s	115640.37	3.6
RAMP method					
Analysis	**Mesh**	**Number of iterations**	**Processing Time**	**Compliance (J)**	**Filter radius (cm)**
No filter	40x40	272	2s	4434.37	0
	80x80	692	35s	17241.14	0
	160x160	894	6min 38s	67478.81	0
Sensitivity filter	40x40	278	2s	4714.58	3.6
	80x80	202	10s	19325.52	3.6
	160x160	226	51s	77303.15	3.6
Density filter	40x40	590	5s	5848.89	3.6
	80x80	1640	1min 41s	24364.83	3.6
	160x160	2546	20min 6s	98444.69	3.6

Mesh 40x40   **Mesh 80x80**   **Mesh 160x160**
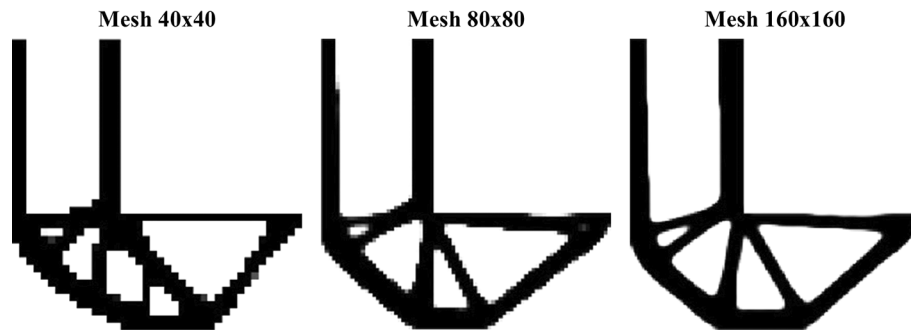
Figure 20. Optimized topologies for the L-bracket beam employing the top99neo algorithm.

non-filtering strategy is performed. In general, the RAMP method has been shown to efficiently produce checkerboard-free optimized topologies with lower values for structural compliance. Thus, these results demonstrate the proposed approach's efficiency and justify its use in topology optimization problems of continuum elastic structures since it better controls numerical issues associated with checkerboard and length scale. The filter radius is slightly higher than $1.01\sqrt{l_q^2 + h_q^2}$ for the coarse mesh. As a result, the filter guarantees the absence of mesh dependency, especially when the RAMP method or the sensitivity filter are employed.
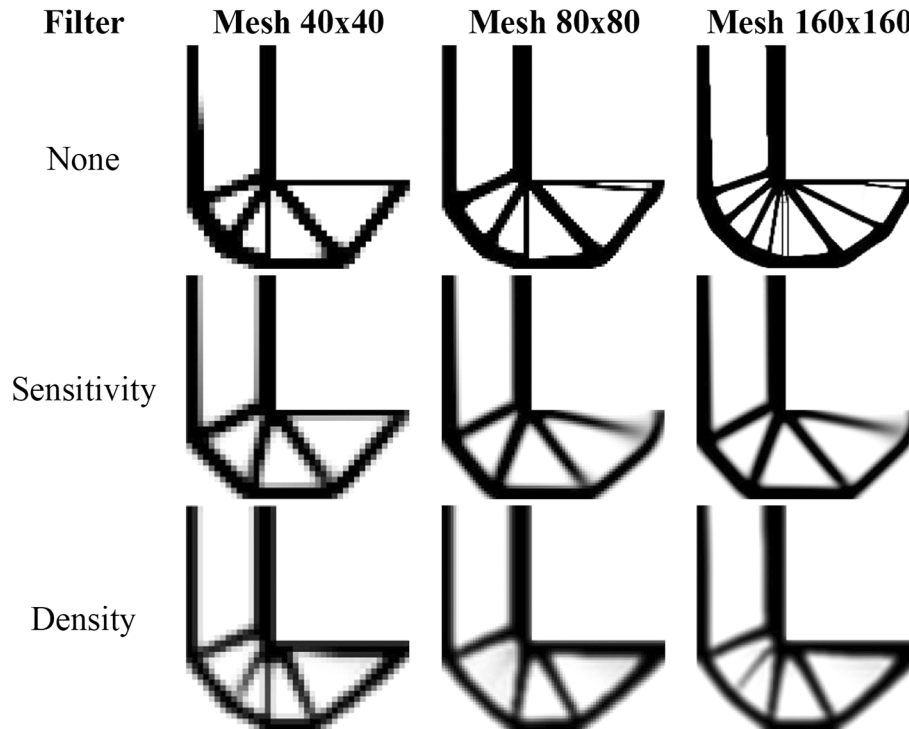
Figure 21. **Optimized topologies for the L-bracket beam obtained by the RAMP approach.**

7. Conclusions

This study introduces the Top2DFVT, an innovative Matlab algorithm tailored for the topology optimization of two-dimensional elastic structures via the finite-volume theory. This contribution addresses compliance minimization problems, presenting a checkerboard-free methodology that mitigates numerical instabilities like mesh dependence and local minima, commonly encountered in gradient-based optimization techniques. The algorithm showcases improved computational efficiency and the ability to generate optimized topologies for medium to large-scale problems by employing two material interpolation schemes, SIMP and RAMP, alongside sensitivity and density filters. Such advancements facilitate the design of high-performance structures with potential applications in various engineering domains.

This algorithm can provide checkerboard-free optimized topologies and reduce mesh dependence or length scale issues, mainly when the RAMP method is employed. The optimized topologies obtained without filtering techniques for the coarse meshes and employing the RAMP method are similar to those obtained with filtering strategies for the finer meshes. Usually, filtering techniques are based on image processing that geometrically changes the sensitivity or the relative density values. Therefore, obtaining optimized structures without filtering techniques provides more reliable and efficient designs. Besides, the optimized topologies without filtering strategies are well-defined "black and white" designs, where intermediate values of relative densities are reduced.

The approach based on the finite-volume theory is also performed by employing a sensitivity filter to solve problems related to mesh dependence and length scale issues. The adopted strategy to define the filter radius consists of using approximately the subvolume's or element's diagonal of the coarse mesh. The continued penalization scheme is adopted for the compliance minimization problem, which guarantees a gradual convergence for the overall process. When the SIMP method is employed, the OC method's damping factor can be adjusted to $1/2.6$ to avoid divergence during the optimization process, especially when non-filtering strategies are employed.

Although the finite-volume theory employed in the TOP2DFVT algorithm effectively mitigates checkerboard patterns, filtering techniques remain essential for producing manufacturable designs. Filters such as sensitivity and density filters play a crucial role in controlling the characteristic length scale, thereby reducing the formation of thin structural elements that could cause fabrication and structural stability challenges. Additionally, applying these filters contributes to a smoother distribution of material, resulting in a more uniform stress distribution across the structure.

However, results obtained without filters can also be explored effectively within the finite-volume theory framework. When working with coarser meshes, the larger subvolumes naturally limit the appearance of thin elements, which helps to define a more favorable topology from a manufacturing perspective. These larger subvolumes act as a resolution control mechanism, preventing the appearance of fine bars that could lead to structural issues such as localized buckling or stress concentration. Thus, the finite-volume theory provides a flexible approach for generating optimized topologies that balance manufacturability and structural robustness by carefully selecting the mesh size and employing or omitting filters as appropriate.

In topology optimization without filters, distinct "black and white" designs can typically be achieved, representing clear material and void regions. When filters such as sensitivity or density filters are applied, gray regions often emerge in the design. These gray elements represent intermediate density values that compromise the binary nature of the solution. To mitigate this issue and increase the discreteness of the topology, volume-preserving Heaviside projection is a commonly used strategy. The Heaviside projection function sharpens the transition between material and void by pushing intermediate densities towards 0 or 1, thereby reducing the gray regions. This technique preserves the total volume while enhancing the manufacturability of the optimized structure (Bendsøe and Sigmund 2003; Ferrari and Sigmund 2020). Future implementations of the proposed method could benefit from incorporating the Heaviside projection to refine the design's discreteness further and improve its practical applicability in manufacturing processes, especially when employing filtering techniques.

In conclusion, this study presents a novel approach to topology optimization using the finite-volume theory and significantly contributes to the field by addressing and overcoming inherent numerical challenges. The Top2DFVT algorithm represents a pivotal advancement in optimizing elastic structures, promising more reliable and efficient design solutions. The authors' efforts in developing and sharing this tool underscore the collaborative spirit of the research community, aiming to broaden the understanding and application of topology optimization in engineering.

This work sets a new benchmark for future research, encouraging further exploration and development of optimization techniques. By providing a robust and efficient tool in Top2DFVT, the authors offer valuable resources for educators, researchers, and practitioners alike, fostering innovation and excellence in engineering design.

Ethics and consent
Ethical approval and consent were not required.

Data availability
No data are associated with this article.

Software availability
All the presented results can be reproduced using the codes available in the GitHub links (https://github.com/fvt7782/Top2DFVT, for Matlab implementation, and https://github.com/fvt7782/Top2DFVT_Oct, for GNU Octave implementation) and by following the instructions presented in this article. For the GNU Octave implementation, the fsparse speedup is not available. The alternative version of the code using the GNU Octave platform has a few changes compared to the original Matlab code. The processing times for the GNU Octave code are higher than those for the Matlab code, but all the optimized topologies shown in the article can be generated with the GNU Octave code.

- **Source code available from**: https://github.com/fvt7782/Top2DFVT, for Matlab implementation, and https://github.com/fvt7782/Top2DFVT_Oct, for GNU Octave implementation.

- **Archived source code at time of publication**: https://doi.org/10.5281/zenodo.11391501, for Matlab implementation, and https://doi.org/10.5281/zenodo.12551626, for GNU Octave implementation.

- **Licenses**: The 2-Clause BSD License and CC-BY 4.0.

References

Aage N, Andreassen E, Lazarov BS: **Topology optimization using PETSc: An easy-to-use, fully parallel, open-source topology optimization framework.** *Struct. Multidiscip. Optim.* 2015; **51**: 565–572.
Publisher Full Text

Aage N, Jørgensen MN, Andreasen CS, *et al*.: **Interactive topology optimization on hand-held devices.** *Struct. Multidiscip. Optim.* 2013; **47**: 1–6.
Publisher Full Text

Aage N, Lazarov BS: **Parallel framework for topology optimization using the method of moving asymptotes.** *Struct. Multidiscip. Optim.* 2013; **47**: 493–505.
Publisher Full Text

Almeida JHS Jr, Christoff BG, Tita V, *et al*.: **A concurrent fibre orientation and topology optimisation framework for 3D-printed fibre-reinforced composites.** *Compos. Sci. Technol.* 2023; **232**: 109872.
Publisher Full Text

Andreassen E, Clausen A, Schevenels M, *et al*.: **Efficient topology optimization in Matlab using 88 lines of code.** *Struct. Multidiscip. Optim.* 2011; **43**(1): 1–16.
Publisher Full Text

Araujo MVO, Lages EN, Cavalcante MAA: **Checkerboard free topology optimization for compliance minimization applying the finite-volume theory.** *Mech. Res. Commun.* 2020a; **108**: 103581.
Publisher Full Text

Araujo MVO, Lages EN, Cavalcante MAA: **Checkerboard-free topology optimization for compliance minimization of continuum elastic structures based on the generalized finite-volume theory.** *Lat. Am. J. Solids Struct.* 2020b; **17**(8): 1–21.
Publisher Full Text

Araujo MVO, Lages EN, Cavalcante MAA: **Energy analysis of continuum elastic structures by the generalized finite-volume theory.** *Acta Mech.* 2021; **232**: 4625–4643.
Publisher Full Text

Arruda LS, Martim MB, Góis W, *et al*.: **Topology optimization – unconventional approaches using the generalized finite element method and the stable generalized finite element method.** *Lat. Am. J. Solids Struct.* 2022; **19**(3): 1–17.

Bendsøe MP: *Optimization of structural topology shape and material.* New York: Springer; 1995.

Bendsøe MP, Kikuchi N: **Generating optimal topologies in structural design using a homogenization method.** *Comput. Methods Appl. Mech. Eng.* 1988; **71**(2): 197–224.
Publisher Full Text

Bendsøe MP, Sigmund O: *Topology optimization: Theory, methods, and applications.* 2nd ed. Berlin, Heidelberg: Springer; 2003.
Publisher Full Text

Borrvall T, Petersson J: **Large-scale topology optimization in 3D using parallel computing.** *Comput. Methods Appl. Mech. Eng.* 2001; **190**(46-47): 6201–6229.
Publisher Full Text

Bouajila W, Furusawa D, Shimoda M: **Multidisciplinary free-form optimization of solid structures for mean compliance minimization and time-dependent temperature control.** *Struct. Multidiscip. Optim.* 2021; **63**(5): 2305–2324.
Publisher Full Text

Cavalcante MAA, Marques SPC, Pindera M-J: **Parametric formulation of the finite-volume theory for functionally graded materials – Part I: analysis.** *J. Appl. Mech.* 2007a; **74**(5): 935–945.
Publisher Full Text

Cavalcante MAA, Marques SPC, Pindera M-J: **Parametric formulation of the finite-volume theory for functionally graded materials – Part II: numerical results.** *J. Appl. Mech.* 2007b; **74**(5): 946–957.
Publisher Full Text

Cavalcante MAA, Marques SPC, Pindera M-J: **Computational aspects of the parametric finite-volume theory for functionally graded materials.** *Comput. Mater. Sci.* 2008; **44**(2): 422–438.
Publisher Full Text

Cavalcante MAA, Pindera M-J: **Generalized finite-volume theory for elastic analysis in solid mechanics – part I: framework.** *J. Appl. Mech.* 2012a; **79**(5): 051006.
Publisher Full Text

Cavalcante MAA, Pindera M-J: **Generalized finite-volume theory for elastic analysis in solid mechanics – part II: results.** *J. Appl. Mech.* 2012b; **79**(5): 051007.
Publisher Full Text

Deaton JD, Grandhi RV: **A survey of structural and multidisciplinary continuum topology optimization: post 2000.** *Struct. Multidiscip. Optim.* 2014; **49**: 1–38.
Publisher Full Text

Engblom S, Lukarski D: **Fast Matlab compatible sparse assembly on multicore computers.** *Parallel Comput.* 2016; **56**: 1–17.
Publisher Full Text

Ferrari F, Sigmund O: **A new generation 99 line Matlab code for compliance topology optimization and its extension to 3D.** *Struct. Multidiscip. Optim.* 2020; **62**(4): 2211–2228.
Publisher Full Text

Kumar P: **HoneyTop90: A 90-line Matlab code for topology optimization using honeycomb tessellation.** *Optim. Eng.* 2023; **24**: 1433–1460.
Publisher Full Text

Lee S, Lieu QX, Vo TP, *et al*.: **Topology optimization using super-resolution image reconstruction methods.** *Adv. Eng. Softw.* 2023; **177**: 103413.
Publisher Full Text

Liu K, Tovar A: **An efficient 3D topology optimization code written in Matlab.** *Struct. Multidiscip. Optim.* 2014; **50**: 1175–1196.
Publisher Full Text

Liu Y, Lai Z, Lu Y, *et al*.: **Topology optimization of shell-infill structures considering buckling constraint.** *Comput. Struct.* 2023; **283**: 107055.
Publisher Full Text

Liu Z, Korvink JG, Huang I: **Structure topology optimization: fully coupled level set method via FEMLAB.** *Struct. Multidiscip. Optim.* 2005; **29**(29): 407–417.
Publisher Full Text

Ma Z-D, Kikuchi N, Hagiwara I: **Structural topology and shape optimization for a frequency response problem.** *Comput. Mech.* 1993; **13**(3): 157–174.
Publisher Full Text

Michell AGM: **The limits of economy of material in frame structures.** *The London, Edinburg, and Dublin Philosophical Magazine and Journal of Science.* 1904; **8**(47): 589–597.
Publisher Full Text

Montes MA: *Topology optimization algorithms for the solution of compliance and volume problems in 2D.* Mexico: Investigation Center in Mathematics; 2016. Master Thesis.

Rozvany GIN: **A critical review of established methods of structural topology optimization.** *Struct. Multidiscip. Optim.* 2009; **37**(3): 217–237.
Publisher Full Text

Sigmund O: **A 99 line topology optimization code written in Matlab.** *Struct. Multidiscip. Optim.* 2001; **21**(2): 120–127.
Publisher Full Text

Sigmund O: **Morphology-based black and white filters for topology optimization.** *Struct. Multidiscip. Optim.* 2007; **33**(4-5): 401–424.
Publisher Full Text

Smit T, Aage N, Ferguson SJ, *et al*.: **Topology optimization using PETSc: a Python wrapper and extended functionality.** *Struct. Multidiscip. Optim.* 2021; **64**: 4343–4353.
Publisher Full Text

Sokół T: **A 99 line code for discretized Michell truss optimization written in Mathematica.** *Struct. Multidiscip. Optim.* 2011; **43**(2): 181–190.
Publisher Full Text

Stolpe M, Svanberg K: **An alternative interpolation scheme for minimum compliance topology optimization.** *Struct. Multidiscip. Optim.* 2001; **22**(2): 116–124.
Publisher Full Text

Stutz FC, Olsen TF, Groen JP, *et al*.: **Synthesis of frame field-aligned multi-laminar structures.** *ACM Trans. Graph.* 2022; **41**(5): 1–20.
Publisher Full Text

Talischi C, Paulino GH, Pereira A, *et al*.: **PolyTop: a Matlab implementation of a general topology optimization framework using unstructured polygonal finite-element meshes.** *Struct. Multidiscip. Optim.* 2012; **45**: 329–357.
Publisher Full Text

Tavakoli R, Mohseni SM: **Alternating active-phase algorithm for multimaterial topology optimization problems: a 115-line Matlab implementation.** *Struct. Multidiscip. Optim.* 2014; **49**: 621–642.
Publisher Full Text

Wei P, Li Z, Li X, *et al*.: **An 88-line Matlab code for the parameterized level set method based topology optimization using radial basis functions.** *Struct. Multidiscip. Optim.* 2018; **58**: 831–849.
Publisher Full Text

Yi B, Yoon GH, Zheng R, *et al*.: **A unified material interpolation for topology optimization of multi-materials.** *Comput. Struct.* 2023; **282**: 107041.
Publisher Full Text

Zegard T, Paulino GH: **GRAND — Ground structure-based topology optimization for arbitrary 2D domains using Matlab.** *Struct. Multidiscip.*

Optim. 2014; **50**: 861–882.
Publisher Full Text

Zhou M, Sigmund O: **Complementary lecture notes for teaching the 99/88-line topology optimization codes.** *Struct. Multidiscip. Optim.* 2021; **64**: 3227–3231.
Publisher Full Text

Zhuang Z, Xie YM, Li Q, *et al*.: **A 172-line Matlab code for structural topology optimization in the body-fitted mesh.** *Struct. Multidiscip. Optim.* 2023; **66**: 11.
Publisher Full Text

Open Peer Review

Current Peer Review Status: ✔ ✔ ✔

Version 2

Reviewer Report 30 October 2024

https://doi.org/10.5256/f1000research.173411.r333833

✔ **Volnei Tita** (iD)

University of Sao Paulo, Sao Paulo, Brazil

I do not have further comments to make.

Competing Interests: No competing interests were disclosed.

Reviewer Expertise: Computational Analysis of Composite Structures

I confirm that I have read this submission and believe that I have an appropriate level of expertise to confirm that it is of an acceptable scientific standard.

Reviewer Report 29 October 2024

https://doi.org/10.5256/f1000research.173411.r333832

✔ **Minh Ngoc Nguyen** (iD)

Duy Tan Research Institute for Computational Engineering, Duy Tan University, Ho Chi Minh city, Vietnam

The authors have addressed all of my comments.

Competing Interests: No competing interests were disclosed.

Reviewer Expertise: Topology optimization

I confirm that I have read this submission and believe that I have an appropriate level of expertise to confirm that it is of an acceptable scientific standard.

Reviewer Report 26 October 2024

https://doi.org/10.5256/f1000research.173411.r333831

✔ **Yingjun Wang** iD

South China University of Technology, Guangzhou, Guangdong, China

The authors have addressed all of my comments.

Competing Interests: No competing interests were disclosed.

Reviewer Expertise: topology optimization

I confirm that I have read this submission and believe that I have an appropriate level of expertise to confirm that it is of an acceptable scientific standard.

- -

Version 1

Reviewer Report 04 September 2024

https://doi.org/10.5256/f1000research.165561.r313235

? **Volnei Tita** iD

University of Sao Paulo, Sao Paulo, Brazil

The paper consists of providing a MATLAB code based on Finite-Volume Theory (named Top2DFVT), which can perform 2D topology optimization of structures by using SIMP and RAMP algorithms. On one hand, the manuscript brings relevant results, mitigating some numerical instabilities, such as checkerboard and mesh dependence issues. By another hand, there are some important aspects related to the manuscript and to the implemented code, which need to be better clarified by the authors as follows:
(*) 1. Introduction
- The authors claim that "...this is the first time a platform for optimizing structures using the finite-

volume theory...". It is very hard to confirm that there is not any work in the World previously published in a journal or conference in this field. Thus, it is recommended that the authors modify the text by the inclusion of "Based on the authors' knowledge, this is the first time a platform...".
- The authors mentioned about computational cost, comparing the previous version of the code approached in Araujo et al. (2020a) with the present one. However, it would be very important to compare and discuss advantages and disadvantages with other codes. For example, usually, FORTRAN codes run faster than MALTAB codes. In fact, in the final of Section 5, the authors presented some advantages, but it is not possible to find drawbacks.
(*) 2. Finite-volume theory
- In the Eq (4), K is a non-symmetric matrix, then the computational cost of topology optimization based on the FVT is higher than based on the FEM. The authors should comment quantitative values, expressing how slow is the process based on the FVT.
(*) 6. Numerical results
- The authors analyzed 3 Case Studies (cantilever deep beam; half MBB beam; L-bracket beam) to show the potentialities of the developed MATLAB code. But they are invited to analyze one of the case studies presented in the paper cited below:
A concurrent fibre orientation and topology optimisation framework for 3D-printed fibre-reinforced composites -
(Almeida Jr. J, et al., 2023 [Ref 1])
In other words, they should compare the results obtained by the Top2DFVT with the results discussed in the paper.

References

1. Almeida Jr. J, Christoff B, Tita V, St-Pierre L: A concurrent fibre orientation and topology optimisation framework for 3D-printed fibre-reinforced composites. *Composites Science and Technology*. 2023; **232**. Publisher Full Text

Is the work clearly and accurately presented and does it cite the current literature?

Yes

Is the study design appropriate and is the work technically sound?

Yes

Are sufficient details of methods and analysis provided to allow replication by others?

Yes

If applicable, is the statistical analysis and its interpretation appropriate?

Not applicable

Are all the source data underlying the results available to ensure full reproducibility?

Yes

Are the conclusions drawn adequately supported by the results?

Yes

Competing Interests: No competing interests were disclosed.

Reviewer Expertise: Computational Analysis of Composite Structures

I confirm that I have read this submission and believe that I have an appropriate level of expertise to confirm that it is of an acceptable scientific standard, however I have significant reservations, as outlined above.

Author Response 13 Oct 2024

Marcio Cavalcante

The authors have many thanks to the reviewer for their valuable comments. The manuscript has been revised in accordance with the comments, and detailed revisions are listed below point by point.

Comments to the Authors:
The paper consists of providing a MATLAB code based on Finite-Volume Theory (named Top2DFVT), which can perform 2D topology optimization of structures by using SIMP and RAMP algorithms. On one hand, the manuscript brings relevant results, mitigating some numerical instabilities, such as checkerboard and mesh dependence issues. By another hand, there are some important aspects related to the manuscript and to the implemented code, which need to be better clarified by the authors as follows:
1) Introduction
- The authors claim that "…this is the first time a platform for optimizing structures using the finite-volume theory…". It is very hard to confirm that there is not any work in the World previously published in a journal or conference in this field. Thus, it is recommended that the authors modify the text by the inclusion of "Based on the authors' knowledge, this is the first time a platform…".
Response: The authors agreed with the reviewer, and the following modification was made to the manuscript:
In addition, **based on the authors' knowledge,** this is the first time a platform for optimizing structures using the finite-volume theory can be applied to medium and large-scale problems, besides obtaining checkerboard-free and mesh-independent designs.

1) Introduction
- The authors mentioned about computational cost, comparing the previous version of the code approached in Araujo et al. (2020a) with the present one. However, it would be very important to compare and discuss advantages and disadvantages with other codes. For example, usually, FORTRAN codes run faster than MALTAB codes. In fact, in the final of Section 5, the authors presented some advantages, but it is not possible to find drawbacks.
Response: The authors agreed with the reviewer, and the following texts and figures were added to the manuscript with results obtained by the top99neo algorithm, discussing the advantages and disadvantages of the Top2DFVT code:
The algorithm known as top99neo, proposed by Ferrari and Sigmund in 2020, is used as a benchmark source for the traditional finite-element method for bilinear elements. The algorithm uses the continued penalization scheme, gradually increasing the penalty factor ($\Delta p=0.25$) from 1 to 4, similar to the finite-volume theory approach. Each penalty factor is subjected to 25 iterations. The Heaviside projection parameters are updated throughout the optimization process. The parameter β starts at 2 and increases to 16 by an increment of

△β=2 every 25 iterations. Figure 12 shows the optimized topologies obtained using the density filter. The filter radius changes to reflect the exact size of the filter radius employed in the finite-volume theory approaches for each mesh size (1.5, 3, and 6, respectively). The optimized topologies obtained using the finite-element approach are more mesh-dependent, even when filtering strategies are employed, as compared to the optimized topologies obtained using the finite-volume theory approach, especially in the case of the results with the sensitivity filter. The computational cost for the finest mesh is 2 minutes and 30 seconds, with a maximum of 350 iterations. The total number of degrees of freedom for the finite-element approach is 132132, while the finite-volume theory approach has a total of 260280 degrees of freedom, which partially explains the difference in computational costs. As the top99neo algorithm employs finite elements with unitary dimensions, it is not feasible to compare the obtained values for the objective function of the optimized topologies.

See Figure 12. Optimized topologies for the cantilever deep beam employing the top99neo algorithm.(URL)

Figure 16 shows the optimized topologies obtained employing the top99neo algorithm, where the penalty factor increases gradually (△p=0.25) from 1 to 4 after every 25 iterations until a maximum of 350 iterations, and the beta parameter increases gradually from 2 to 16 (△β=2), after every 25 iterations, similarly to the cantilever deep beam example. The optimized topologies shown in Figure 16 are mesh dependents even when filtering strategies are employed. The filter radius is assumed to be 1.5 for the 90x30 mesh, 3 for the 180x60 mesh, and 6 for the 360x120 mesh. When a similar filter radius is employed in the context of the finite-volume theory, this technique demonstrates a less mesh sensitivity behavior when compared to finite element-based strategies. Regarding computational efficiency, the top99neo code has presented a processing time of 86 seconds for the finest mesh. Generally, the Top2DFVT algorithm presents a higher computational cost when compared to the Q4 finite element-based algorithm. The number of degrees of freedom partially explains this higher computational cost once the total number of degrees of freedom for the finest mesh considering the top99neo algorithm is 87362, while in the Top2DFVT algorithm, the total number of degrees of freedom for the same analysis is 173760. Furthermore, the number of iterations for this example is relatively high for the finite-volume theory approaches once the top99neo algorithm adopts a maximum of 350 iterations.

See Figure 16. Optimized topologies for the MBB beam employing the top99neo algorithm.(URL)

The top99neo algorithm is also performed considering the L-bracket beam problem, and the obtained optimized topologies can be observed in Figure 20. As in the previous examples, the same numerical parameters are employed for the physical model, such as the gradual increase in the penalty factor, from 1 to 4 with △p=0.25, and in the Heaviside Projection β parameter, from 2 to 16 with △β=2. In terms of computational cost, the top99neo code has presented a processing time of 1 minute and 1 second for the finest mesh, considering a total of 350 iterations, while the Top2DFVT algorithm has presented a processing time of 39 seconds with a total of 155 iterations for of the SIMP method and the

sensitivity filter. This difference in processing time can be partially explained by the difference in the total number of iterations observed during the topology optimization analyses. For this example, the Top2DFVT algorithm, considering the sensitivity filter approach, presents a reduced number of iterations for convergence.

See Figure 20. Optimized topologies for the L-bracket beam employing the top99neo algorithm.(URL)

2. Finite-volume theory
- In the Eq (4), K is a non-symmetric matrix, then the computational cost of topology optimization based on the FVT is higher than based on the FEM. The authors should comment quantitative values, expressing how slow is the process based on the FVT.
Response: The local stiffness matrix in Eq. (4) is non-symmetric, which can lead to higher computational costs compared to FEM-based approaches. To address this, we adopted a modified symmetric stiffness matrix, as shown in Eq. (5), motivated by physical considerations. Specifically, the modified local stiffness matrix allows the adoption of energetically conjugated quantities, i.e., the surface-averaged displacements and the resultant forces acting on the subvolume faces. To clarify this, the following text was added to the manuscript:
The modified global stiffness matrix allows the adoption of energetically conjugated quantities, i.e., the surface-averaged displacements and the resultant forces acting on the subvolume faces. This adjustment not only guarantees better physical consistency but also improves computational efficiency by enabling the use of solvers optimized for symmetric systems. As a result, the time required to solve the modified global system of equations is significantly reduced, bringing the computational cost closer to the finite element method-based approaches while retaining the benefits of the finite-volume theory in terms of numerical stability and checkerboard-free solutions.

6. Numerical results
- The authors analyzed 3 Case Studies (cantilever deep beam; half MBB beam; L-bracket beam) to show the potentialities of the developed MATLAB code. But they are invited to analyze one of the case studies presented in the paper cited below:
A concurrent fibre orientation and topology optimisation framework for 3D-printed fibre-reinforced composites - (Almeida Jr. J, et al., 2023 [Ref 1])
In other words, they should compare the results obtained by the Top2DFVT with the results discussed in the paper.
Response: The authors appreciate the reviewer's suggestion to include an additional case study based on the work of Almeida et al. (2023). While their paper presents noteworthy results, particularly in the concurrent optimization of fibre orientation and topology for 3D-printed composites, the authors have opted not to expand the scope of the current manuscript with further case studies. The focus of this article is to present the capabilities of the Top2DFVT code within the context of traditional isotropic materials, and the authors believe the selected case studies effectively demonstrate the tool's potential.
However, the authors recognize the value of comparing results with those presented in Almeida et al. (2023) and intend to explore these comparisons in future publications. For now, the authors have chosen to include the following text in the introduction of the manuscript, highlighting recent advancements in topology optimization for anisotropic

composites:
Recent advances in topology optimization have expanded to include anisotropic composites, optimizing both material distribution and fibre orientation. Almeida et al. (2023) introduced a framework for concurrent optimization of topology and fibre orientation in 3D-printed fibre-reinforced composites, effectively minimizing compliance. This approach, particularly for materials like onyx, enhances stiffness and strength, offering significant benefits for additive manufacturing of high-performance and lightweight structures.
Added reference:
Almeida JHS Jr, Christoff BG, Tita V, St-Pierre L. A concurrent fibre orientation and topology optimisation framework for 3D-printed fibre-reinforced composites. Composites Science and Technology. 2023;232:109872. doi:10.1016/j.compscitech.2022.109872.

Competing Interests: No competing interests were disclosed.

Reviewer Report 26 August 2024

https://doi.org/10.5256/f1000research.165561.r313232

?

Minh Ngoc Nguyen 🔵
Duy Tan Research Institute for Computational Engineering, Duy Tan University, Ho Chi Minh city, Vietnam

Comments for
Top2DFVT: An efficient Matlab Implementation for topology optimization based on Finite-Volume theory

The manuscript presents a Matlab implementation for topology optimization based on Finite Volume theory for 2D compliance problems.
In general, the manuscript is interesting and is very useful for beginners of topology optimization. The Matlab code is fast, due to vectorization and memory pre-allocation, in a manner similar to the code top88 (Andreassen E, et al., 2011 [Ref 1]). Compared to the previous works by the same group of authors, computational time is reduced significantly. However, there are many unclear information that needs thorough revision by the authors
1. Although the approach may not require filter to avoid checkerboard pattern, it is clearly observed in the results that when no filter is applied, many thin components appear in the optimized design. Such thin components may be suffered from high stress values. In fact, as in the literature, filter also contributes to length-scale control. The authors should discuss this aspect.
2. When there is no filter, it seems that clear "black and white" results could be obtained. Nevertheless, the authors should compute the non-discreteness values to quantitatively demonstrate this aspect.
On the other hand, when filter (either sensitivity filter or density filter) is applied, gray elements

appear. In order to reduce the gray elements and increase the discreteness of the solution, volume-preserving Heaviside projection is commonly employed. The authors should also mention this.

References

1. Andreassen E, Clausen A, Schevenels M, Lazarov B, et al.: Efficient topology optimization in MATLAB using 88 lines of code. *Structural and Multidisciplinary Optimization*. 2011; **43** (1): 1-16
Publisher Full Text

Is the work clearly and accurately presented and does it cite the current literature?
Yes

Is the study design appropriate and is the work technically sound?
Yes

Are sufficient details of methods and analysis provided to allow replication by others?
Yes

If applicable, is the statistical analysis and its interpretation appropriate?
Not applicable

Are all the source data underlying the results available to ensure full reproducibility?
Yes

Are the conclusions drawn adequately supported by the results?
Yes

Competing Interests: No competing interests were disclosed.

Reviewer Expertise: Topology optimization

I confirm that I have read this submission and believe that I have an appropriate level of expertise to confirm that it is of an acceptable scientific standard, however I have significant reservations, as outlined above.

Author Response 13 Oct 2024
Marcio Cavalcante

The authors have many thanks to the reviewer for their valuable comments. The manuscript has been revised in accordance with the comments, and detailed revisions are listed below point by point.

Comments to the Authors:
Reviewer comment: The manuscript presents a Matlab implementation for topology optimization based on Finite Volume theory for 2D compliance problems.
In general, the manuscript is interesting and is very useful for beginners of topology

optimization. The Matlab code is fast, due to vectorization and memory pre-allocation, in a manner similar to the code top88 (Andreassen E, et al., 2011 [Ref 1]). Compared to the previous works by the same group of authors, computational time is reduced significantly. However, there are many unclear information that needs thorough revision by the authors. 1) Although the approach may not require filter to avoid checkerboard pattern, it is clearly observed in the results that when no filter is applied, many thin components appear in the optimized design. Such thin components may be suffered from high stress values. In fact, as in the literature, filter also contributes to length-scale control. The authors should discuss this aspect.

Author response: *The authors agreed with the reviewer, and the following texts were added to the manuscript:*

Although the finite-volume theory employed in the TOP2DFVT algorithm effectively mitigates checkerboard patterns, filtering techniques remain essential for producing manufacturable designs. Filters such as sensitivity and density filters play a crucial role in controlling the characteristic length scale, thereby reducing the formation of thin structural elements that could cause fabrication and structural stability challenges. Additionally, applying these filters contributes to a smoother distribution of material, resulting in a more uniform stress distribution across the structure.

However, results obtained without filters can also be explored effectively within the finite-volume theory framework. When working with coarser meshes, the larger subvolumes naturally limit the appearance of thin elements, which helps to define a more favorable topology from a manufacturing perspective. These larger subvolumes act as a resolution control mechanism, preventing the appearance of fine bars that could lead to structural issues such as localized buckling or stress concentration. Thus, the finite-volume theory provides a flexible approach for generating optimized topologies that balance manufacturability and structural robustness by carefully selecting the mesh size and employing or omitting filters as appropriate.

Reviewer comment: 2) When there is no filter, it seems that clear "black and white" results could be obtained. Nevertheless, the authors should compute the non-discreteness values to quantitatively demonstrate this aspect.

On the other hand, when filter (either sensitivity filter or density filter) is applied, gray elements appear. In order to reduce the gray elements and increase the discreteness of the solution, volume-preserving Heaviside projection is commonly employed. The authors should also mention this.

Author response: *The authors agreed with the reviewer, and the following texts were added to the manuscript:*

In topology optimization without filters, distinct "black and white" designs can typically be achieved, representing clear material and void regions. When filters such as sensitivity or density filters are applied, gray regions often emerge in the design. These gray elements represent intermediate density values that compromise the binary nature of the solution. To mitigate this issue and increase the discreteness of the topology, volume-preserving Heaviside projection is a commonly used strategy. The Heaviside projection function sharpens the transition between material and void by pushing intermediate densities towards 0 or 1, thereby reducing the gray regions. This technique preserves the total volume while enhancing the manufacturability of the optimized structure (Bendsøe and Sigmund 2003; Ferrari and Sigmund 2020). Future implementations of the proposed

method could benefit from incorporating the Heaviside projection to refine the design's discreteness further and improve its practical applicability in manufacturing processes, especially when employing filtering techniques.

Competing Interests: No competing interests were disclosed.

Reviewer Report 12 August 2024

https://doi.org/10.5256/f1000research.165561.r306477

? **Yingjun Wang** 🆔

South China University of Technology, Guangzhou, Guangdong, China

This paper presents a Matlab implementation for 2D topology optimization based on finite-volume method. The Matlab code Top2DFVT uses the loop vectorization and memory preallocation of top88, which is much more efficient than the authors' previous work. Three examples are tested to demonstrate the validity and efficiency of Top2DFVT. However, there are still some comments for the authors.

1. How to calculate the local stiffness matrix for a subvolume q should be given.

2. What is the meaning of the subscripts "pu", "pp", "uu", "up" in Eq.(13).

3. In Section 3.1, there are two cases for the objective function gradient. Is only one of the cases in a subvolume, or the two cases can exist together in a subvolume?

4. In Section 4, an algorithm flowchart of Top2DFVT should be added.

5. In Top2DFVT, the memory preallocation accelerates the computational efficiency, but increases the memory usage. The authors should state this in the paper.

6. For the illustrative example in Figure 5, why are the number of subvolumes in the horizontal and vertical directions set to 202 and 101, not 200 and 100?

7. In Tables 2-4, it can be found that the number of iterations of No filter cases is larger than the Sensitivity filter cases for the same mesh size, why? In addition, the number of iterations is more than 1000 when the number of elements increases, which is too many for the compliance minimization problem. The convergence history should be given for at least one example.

8. The proposed method should be compared with finite-element-based topology optimization methods such as top88 or top99neo in detail to demonstrate its validity and efficiency.

Is the work clearly and accurately presented and does it cite the current literature?
Yes

Is the study design appropriate and is the work technically sound?
Yes

Are sufficient details of methods and analysis provided to allow replication by others?
Yes

If applicable, is the statistical analysis and its interpretation appropriate?
Yes

Are all the source data underlying the results available to ensure full reproducibility?
Partly

Are the conclusions drawn adequately supported by the results?
Yes

Competing Interests: No competing interests were disclosed.

Reviewer Expertise: topology optimization

I confirm that I have read this submission and believe that I have an appropriate level of expertise to confirm that it is of an acceptable scientific standard, however I have significant reservations, as outlined above.

Author Response 13 Oct 2024
Marcio Cavalcante

The authors have many thanks to the reviewer for their valuable comments. The manuscript has been revised in accordance with the comments, and detailed revisions are listed below point by point.

Comments to the Authors:
This paper presents a Matlab implementation for 2D topology optimization based on finite-volume method. The Matlab code Top2DFVT uses the loop vectorization and memory preallocation of top88, which is much more efficient than the authors' previous work. Three examples are tested to demonstrate the validity and efficiency of Top2DFVT. However, there are still some comments for the authors.
1) How to calculate the local stiffness matrix for a subvolume q should be given.
Response: As mentioned in the manuscript, the local stiffness matrix calculation can be found in Araujo et al. (2020a).2)

2) What is the meaning of the subscripts "pu", "pp", "uu", "up" in Eq.(13).
Response: The following description of the submatrices in Eq. (13) was incorporated into

the text:
The subscripts in Eq. (13) reflect the relationship between prescribed and unknown quantities, where the first index refers to forces and the second to displacements. The letter "u" denotes unknown quantities, while "p" represents prescribed ones. Therefore, the submatrix Kpu expresses the coupling between prescribed forces and unknown displacements, while Kpp defines the relationship between prescribed forces and prescribed displacements. Similarly, Kup describes the interaction between unknown forces and prescribed displacements, and Kuu corresponds to the relationship between unknown forces and unknown displacements. This indexing scheme distinguishes between the interactions of prescribed and unknown quantities within the stiffness matrix.

3) In Section 3.1, there are two cases for the objective function gradient. Is only one of the cases in a subvolume, or the two cases can exist together in a subvolume?
Response: The two cases mentioned in section 3.1 refer to the global system of equations that relates the global force vector with the global displacement vector. The following text was added to the manuscript to clarify the case used in the analyzed examples:
The examples analyzed in the following sections are associated with the second case, where a prescribed force is applied, and all the prescribed displacements are zero.

4) In Section 4, an algorithm flowchart of Top2DFVT should be added.
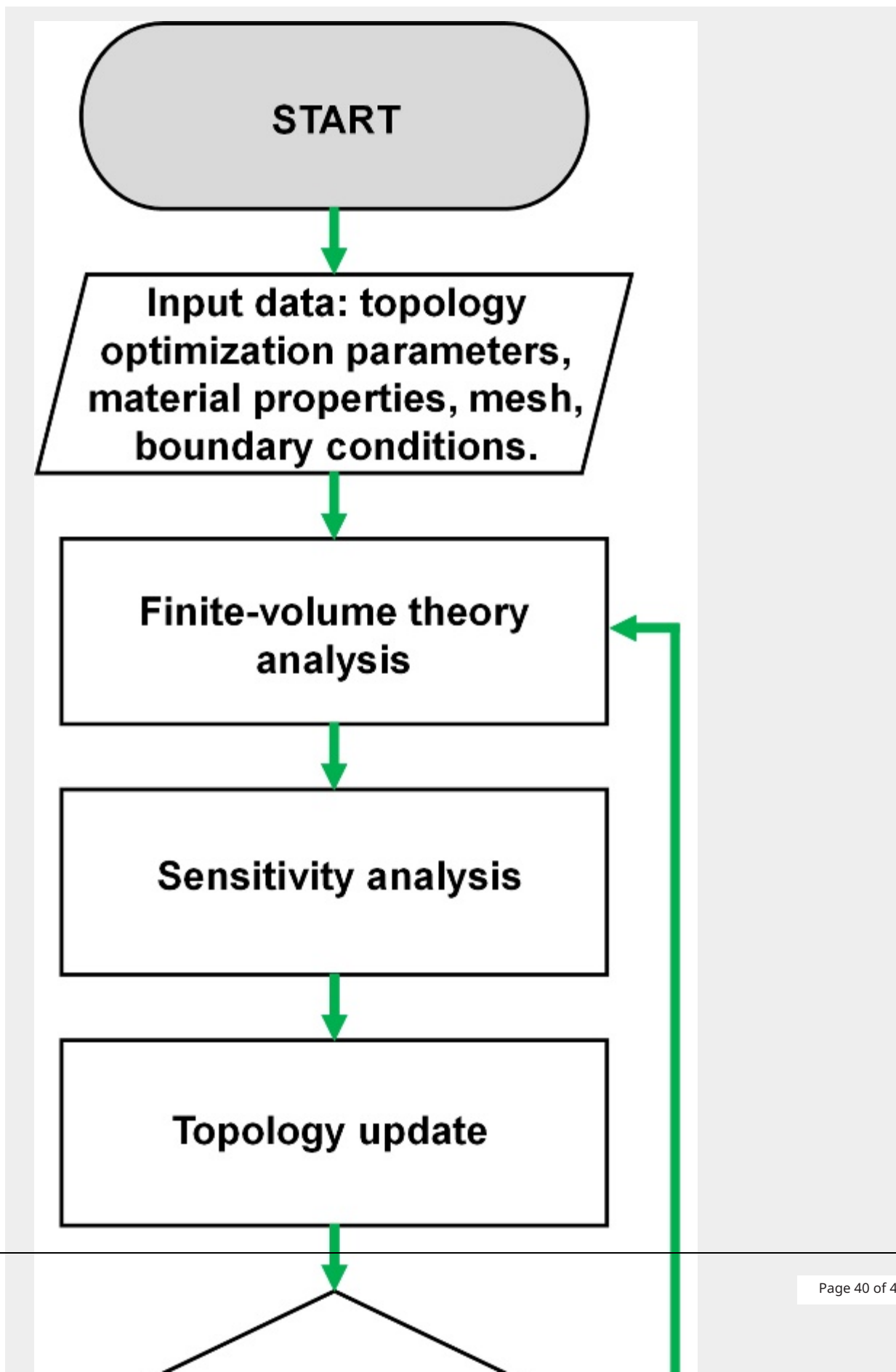*Response: The authors agreed with the reviewer, and the following flowchart was added to the manuscript.*

Figure 4. Flowchart of the Top2DFVT for the topology optimization of linear elastic continuum structures.

5) In Top2DFVT, the memory preallocation accelerates the computational efficiency, but increases the memory usage. The authors should state this in the paper.
Response: The authors agreed with the reviewer, and the following text was added to the manuscript:
In the Top2DFVT implementation, memory preallocation is crucial in enhancing computational efficiency by reducing the time required for matrix assembly and solving linear systems. However, this performance gain comes at the expense of increased memory usage, as large data structures must be allocated in advance. This trade-off between computational speed and memory consumption is a common consideration in the design of topology optimization algorithms. While the memory overhead is manageable for medium-sized problems, it can become significant for large-scale applications. Therefore, careful management of memory resources is essential to balance efficiency and scalability.

6) For the illustrative example in Figure 5, why are the number of subvolumes in the horizontal and vertical directions set to 202 and 101, not 200 and 100?
Response: The following text was added to the manuscript:
In this example, the dimensions of the cantilever deep beam are L=100 and H=50, and the concentrated load is applied at the center of the free edge. To ensure the load is applied to the face of a single subvolume, the number of subvolumes in the vertical direction must be odd. Furthermore, to generate an analysis domain with square subvolumes, the number of subvolumes in the horizontal direction must be twice the number of those in the vertical direction.

7) In Tables 2-4, it can be found that the number of iterations of No filter cases is larger than the Sensitivity filter cases for the same mesh size, why? In addition, the number of iterations is more than 1000 when the number of elements increases, which is too many for the compliance minimization problem. The convergence history should be given for at least one example.
Response: The following text and figure were added to the manuscript:
Adopting the continued penalization scheme, combined with a highly restrictive local convergence criterion, increases the number of iterations in the investigated examples, especially for the most refined meshes, where achieving local convergence is more challenging. The smooth local response produced by the sensitivity filter accelerates convergence compared to the optimization process without filtering techniques, a result not observed with the density filter. Figure 9 displays the objective function histories throughout the optimization process of the cantilever deep beam for the SIMP and RAMP methods, highlighting that the density filter demands more iterations for convergence. In contrast, the optimization process with the sensitivity filter achieves the fastest convergence. The RAMP method provides closer values for the objective function throughout the optimization process for the three approaches adopted: results without filters, with the sensitivity filter, and with the density filter. Furthermore, the RAMP method demonstrates a more stable convergence process than the SIMP method for these approaches. Notably, the jumps in the continued penalization scheme are significantly

smaller for the RAMP method than those between different penalty factors in the SIMP
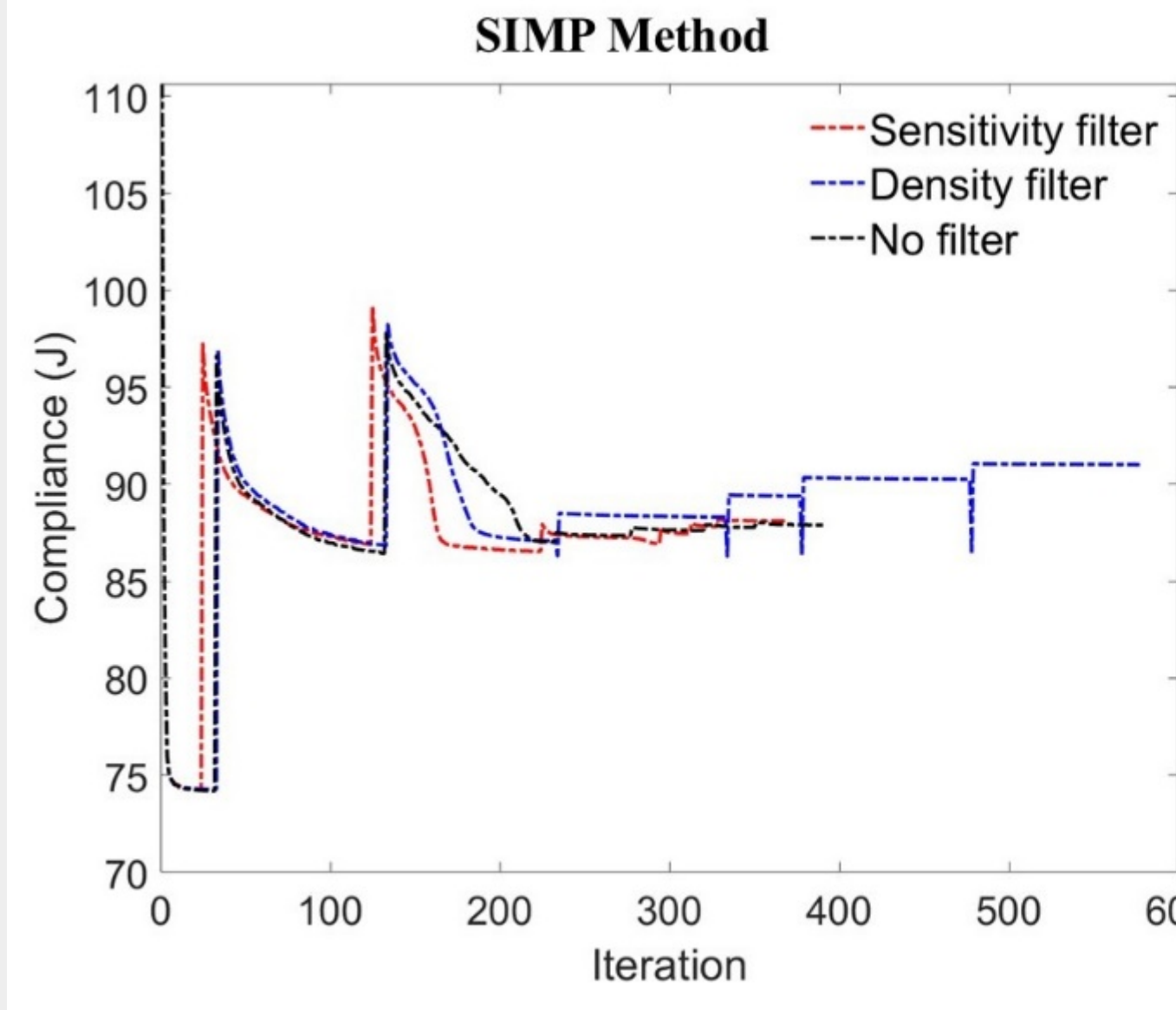method.

SIMP Method

Figure 9. Objective function histories for the SIMP and RAMP methods.

**8) The proposed method should be compared with finite-element-based topology
optimization methods such as top88 or top99neo in detail to demonstrate its validity
and efficiency.**
*Response: The authors agreed with the reviewer, and the following texts and figures were
added to the manuscript:*
The algorithm known as top99neo, proposed by Ferrari and Sigmund in 2020, is used as a
benchmark source for the traditional finite-element method for bilinear elements. The
algorithm uses the continued penalization scheme, gradually increasing the penalty factor (
$\Delta p=0.25$) from 1 to 4, similar to the finite-volume theory approach. Each penalty factor is

subjected to 25 iterations. The Heaviside projection parameters are updated throughout the optimization process. The parameter β starts at 2 and increases to 16 by an increment of Δβ=2 every 25 iterations. Figure 12 shows the optimized topologies obtained using the density filter. The filter radius changes to reflect the exact size of the filter radius employed in the finite-volume theory approaches for each mesh size (1.5, 3, and 6, respectively). The optimized topologies obtained using the finite-element approach are more mesh-dependent, even when filtering strategies are employed, as compared to the optimized topologies obtained using the finite-volume theory approach, especially in the case of the results with the sensitivity filter. The computational cost for the finest mesh is 2 minutes and 30 seconds, with a maximum of 350 iterations. The total number of degrees of freedom for the finite-element approach is 132132, while the finite-volume theory approach has a total of 260280 degrees of freedom, which partially explains the difference in computational costs. As the top99neo algorithm employs finite elements with unitary dimensions, it is not feasible to compare the obtained values for the objective function of the optimized topologies.
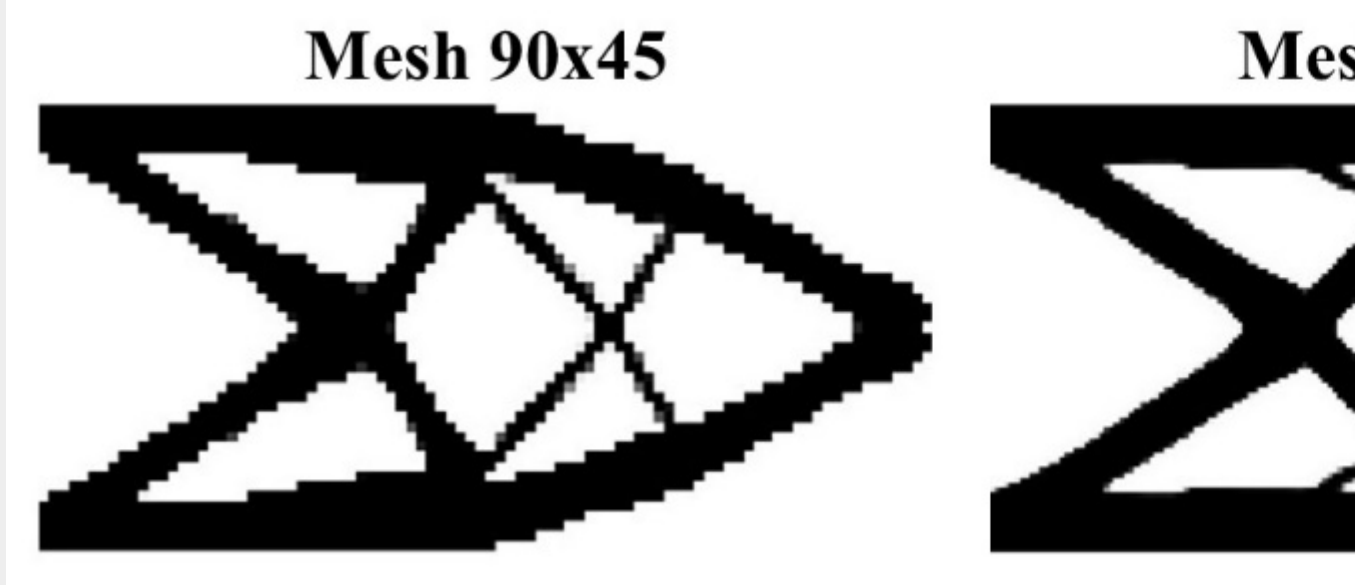

Figure 12. Optimized topologies for the cantilever deep beam employing the top99neo algorithm.

Figure 16 shows the optimized topologies obtained employing the top99neo algorithm, where the penalty factor increases gradually (Δp=0.25) from 1 to 4 after every 25 iterations until a maximum of 350 iterations, and the beta parameter increases gradually from 2 to 16 (Δβ=2), after every 25 iterations, similarly to the cantilever deep beam example. The optimized topologies shown in Figure 16 are mesh dependents even when filtering strategies are employed. The filter radius is assumed to be 1.5 for the 90x30 mesh, 3 for the 180x60 mesh, and 6 for the 360x120 mesh. When a similar filter radius is employed in the context of the finite-volume theory, this technique demonstrates a less mesh sensitivity behavior when compared to finite element-based strategies. Regarding computational efficiency, the top99neo code has presented a processing time of 86 seconds for the finest mesh. Generally, the Top2DFVT algorithm presents a higher computational cost when

compared to the Q4 finite element-based algorithm. The number of degrees of freedom partially explains this higher computational cost once the total number of degrees of freedom for the finest mesh considering the top99neo algorithm is 87362, while in the Top2DFVT algorithm, the total number of degrees of freedom for the same analysis is 173760. Furthermore, the number of iterations for this example is relatively high for the finite-volume theory approaches once the top99neo algorithm adopts a maximum of 350 iterations.
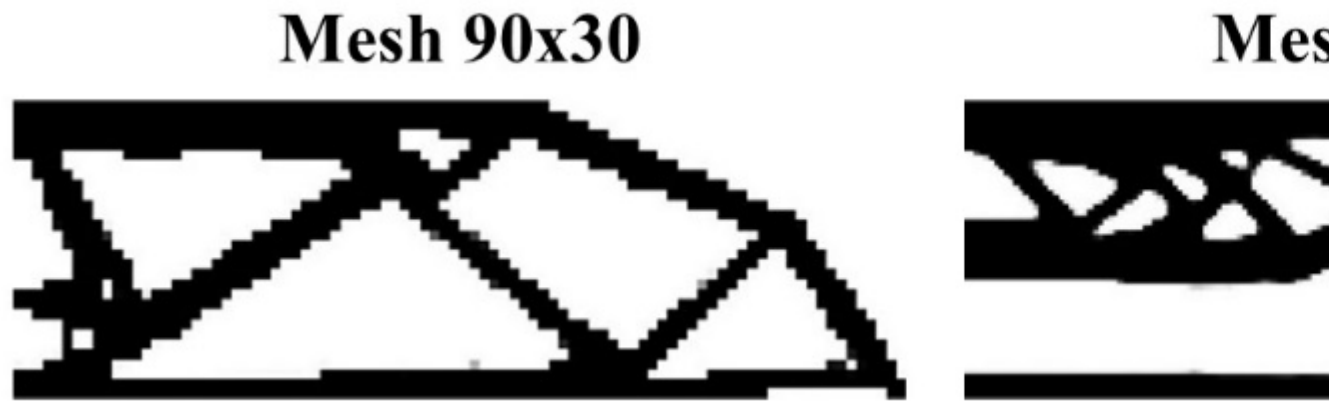

Figure 16. Optimized topologies for the MBB beam employing the top99neo algorithm.

The top99neo algorithm is also performed considering the L-bracket beam problem, and the obtained optimized topologies can be observed in Figure 20. As in the previous examples, the same numerical parameters are employed for the physical model, such as the gradual increase in the penalty factor, from 1 to 4 with $\Delta p=0.25$, and in the Heaviside Projection β parameter, from 2 to 16 with $\Delta\beta=2$. In terms of computational cost, the top99neo code has presented a processing time of 1 minute and 1 second for the finest mesh, considering a total of 350 iterations, while the Top2DFVT algorithm has presented a processing time of 39 seconds with a total of 155 iterations for of the SIMP method and the sensitivity filter. This difference in processing time can be partially explained by the difference in the total number of iterations observed during the topology optimization analyses. For this example, the Top2DFVT algorithm, considering the sensitivity filter approach, presents a reduced number of iterations for convergence.
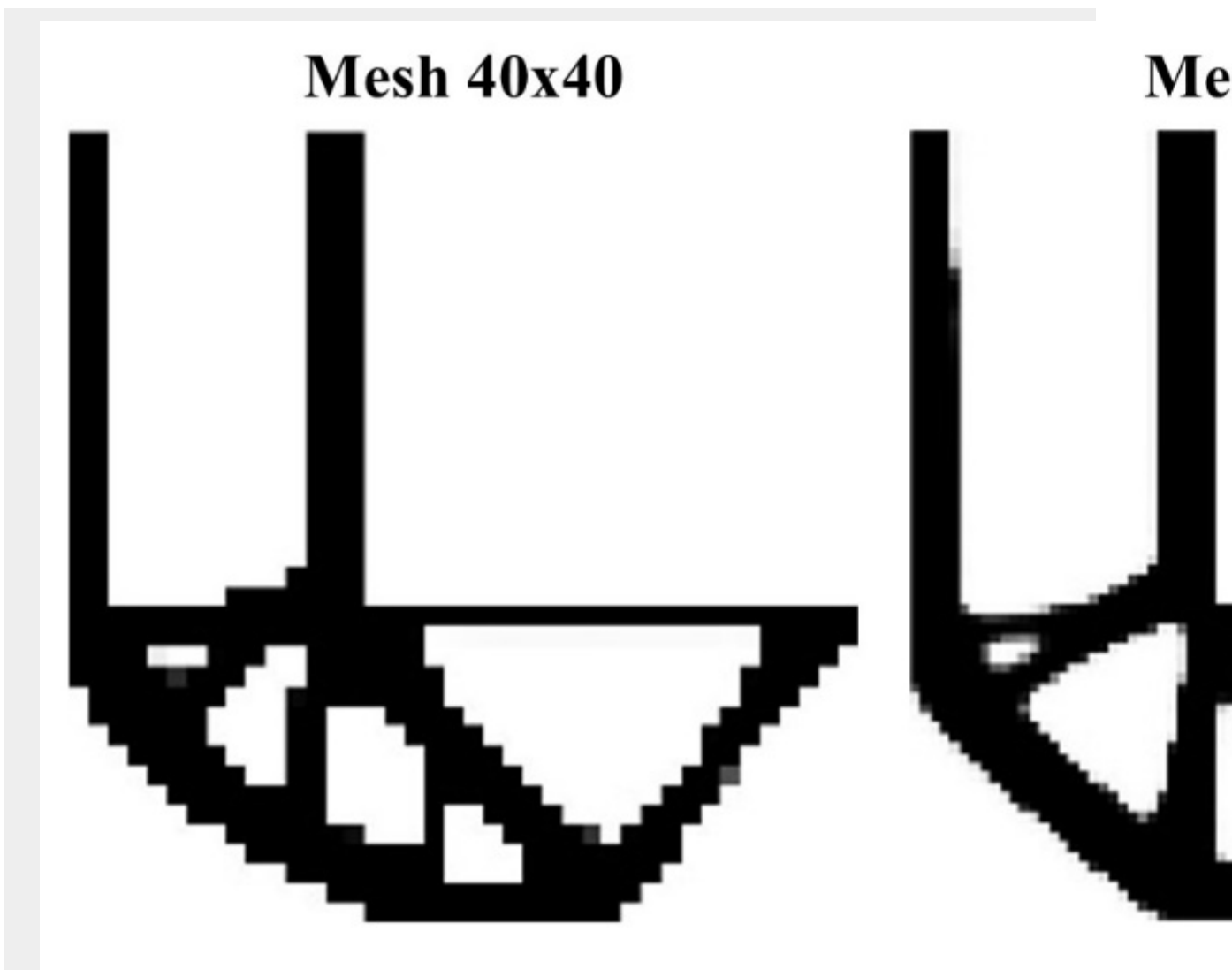
Figure 20. Optimized topologies for the L-bracket beam employing the top99neo algorithm.

Competing Interests: No competing interests were disclosed.

The benefits of publishing with F1000Research:

- Your article is published within days, with no editorial bias

- You can publish traditional articles, null/negative results, case reports, data notes and more

- The peer review process is transparent and collaborative

- Your article is indexed in PubMed after passing peer review

- Dedicated customer support at every stage

For pre-submission enquiries, contact research@f1000.com

F1000Research